Contents lists available at ScienceDirect

Deep-Sea Research Part I

journal homepage: www.elsevier.com/locate/dsri

Gorgoniapolynoe caeciliae revisited: The discovery of new species and molecular connectivity in deep-sea commensal polynoids from the Central Atlantic

Jamie Maxwell [a,b,*], Sergi Taboada [c,d,e], Michelle L. Taylor [b]

[a] *School of Natural Sciences and the Ryan Institute, Martin Ryan Building, National University of Ireland Galway, Galway, Ireland*
[b] *School of Life Sciences, University of Essex, Wivenhoe Park, Colchester, CO4 3SQ, UK*
[c] *Departamento de Biodiversidad, Ecología y Evolución, Facultad de Ciencias Biológicas, Universidad Complutense de Madrid, 28040, Madrid, Spain*
[d] *Life Sciences Department, The Natural History Museum, Cromwell Road, London, SW7 5BD, UK*
[e] *Departamento de Ciencias de la Vida, Apdo. 20, Universidad de Alcalá, 28805, Alcalá de Henares, Spain*

A R T I C L E   I N F O

A B S T R A C T

Gorgoniapolynoe caeciliae (Fauvel, 1913) is a deep-sea commensal polynoid that lives in association with several genera of octocorals from the order Alcyonacea. The species has been recorded in the Caribbean and in both Atlantic and Indian Ocean basins. The wide geographic range of *G. caeciliae,* coupled with it having multiple host coral species and the evolution of its taxonomic description, hints that it could potentially be a species complex. This study investigated the morphological and genetic differentiation in 82 specimens of *G.* cf. *caeciliae,* sampled from four seamounts in the Central Atlantic separated by thousands of kilometres. Our combined morphological and molecular analyses, including species delimitation models (ABGD and bPTP) using *COI* and a phylogenetic approach using four molecular markers (*COI*, *16S*, *28S*, and *18S*), agreed in identifying three distinct species; two supported by morphological and molecular data and a third species, using molecular data only, from the Indian Ocean which had been previously identified as *G. caeciliae.* We formally describe a new species in the genus, *Gorgoniapolynoe pseudocaecliae* sp. nov., the most common taxa found in our study. Our morphological analyses of some members of the genus *Gorgoniapolynoe* revealed the presence of elytra with possible photocytes (bioluminescent cells) and conspicuous macropapillae with long cilia emerging from them, whose function is discussed here. Our demographic analysis using *COI* for two *Gorgoniapolynoe* sp. detected a high potential for dispersal for *G. pseudocaecliae* sp. nov., with sites approximately 3000 km apart being well connected. Unusually there was also no genetic differentiation across their bathymetric range of over 1500 m. All in all, our study highlights the importance of applying integrative taxonomy to poorly studied deep-sea species.

1. Introduction

In the age of molecular analysis, many new deep-sea species are being discovered in previously, seemingly, widespread single species (Vrijenhoek, 2009). These cryptic species were 'hidden' due to a lack of morphological differentiation, the traditional delimiter used by taxonomists since the inception of taxonomy. Even when minor morphological differences between individuals were observed, they were often ascribed to intraspecific variation and plasticity (Castelin et al., 2017; Dueñas and Sánchez, 2009; Oug et al., 2017; Vrijenhoek, 2009). Poor descriptions, due to limited and often damaged holotypes and assumed morphological variation/plasticity, are known to have led to an underestimation of biodiversity in the deep sea (Vrijenhoek, 2009). This underestimation, along with the lack of basic ecological knowledge, is a major barrier towards being able to predict how deep-sea habitats will react under increased anthropogenic pressure from climate change and deep-sea mining (Howell et al., 2020). Marine annelids are a group which have historically been viewed by taxonomists to have high intraspecific morphological variation and wide geographic ranges, particularly deep-sea species (Hutchings and Kupriyanova, 2018). One such species which falls under this description is the deep-sea annelid *Gorgoniapolynoe caeciliae* (Fauvel, 1913).

Gorgoniapolynoe caeciliae, within the family Polynoidae and member of the Suborder Aphroditiformia (Annelida), is a scale worm, named as

---

such due to the presence of scale-like elytra on their dorsal surface. Polynoids are a highly diverse group within scale worms (Gonzalez et al., 2018; Zhang et al., 2018) with over 871 species (Martin et al., 2021). Polynoids are found in all marine habitats but are prominent members of the deep sea, with 16% of all described species found below 1000m (Martin et al., 2021). They are often found in association with other marine taxa in commensal or parasitic symbiotic relationships (Martin and Britayev, 1998, 2018). *Gorgoniapolynoe caeciliae* is a deep-sea commensal species found exclusively in association with deep-sea octocorals from the order Alcyonacea (Fauvel, 1913; Pettibone 1991). They are one of the 490 marine annelid species known to be involved in 1229 commensal relationships with other marine invertebrates (Martin and Britayev, 1998, 2018). All species in the genus *Gorgoniapolynoe* are colonial, meaning many individuals can be found living on a single alcyonacean host (Pettibone 1991). The worms live inside tunnels on coral branches, which are not excavated into the coral, rather the worm appears to induce the coral to modify their sclerites to form these tunnel abodes (Barnich et al., 2013; Pettibone, 1991). Of all the species of *Gorgoniapolynoe*, *G. caeciliae* has accumulated the most records in the literature (Fauvel, 1913; Hartmann-Schroder, 1985; Stock, 1986; Pettibone, 1991; Eckelbarger et al., 2005; Simpson and Watling, 2011; Britayev et al., 2014; Tu et al., 2015; Macpherson et al., 2016; Serpetti et al., 2017). From these studies, *G. caeciliae* has been recorded in association with ten host species of Alcyonacea: *Acanthogorgia armata* Verrill, 1878, *Acanthogorgia aspera* Pourtalès, 1867, *Candidella imbricata* (Johnson, 1862), *Hemicorallium bayeri* (Simpson and Watling, 2011), *Hemicorallium niobe* (Bayer, 1964), *Hemicorallium tricolor* (Johnson, 1899), *Pleurocorallium johnsoni* (Gray, 1860), *Pleurocorallium secundum* (Dana, 1846), *Narella* sp. and Isididae sp.. Among marine annelids, of the 618 symbiotic relationships recorded, 57% are monoxenous i.e., having a single host species, 19% have two host species (polyxenous, having two or more relationships), and in total 33% have between two and five host species (Martin and Britayev, 1998, 2018). Thus, the number of host species recorded for *G. caeciliae* makes it unusual. *Gorgoniapolynoe caeciliae* is also unusual as 72% of known marine annelid associates with deep-sea alcyonacean corals are monoxenous (Molodtsova et al., 2016).

Fauvel (1913) first described *G. caeciliae* (under the synonym *Polynoe caeciliae*) over 100 years ago. There is a significant correlation between the time a deep-sea species is first described and the size of its range (Higgs and Attrill, 2015). Higgs and Attrill (2015) suggested this correlation may be explained due to wide-ranging species being more likely to be encountered earlier and the longer a species has been described, the more records it will accumulate. However, this hypothesis does not explain *G. caeciliae*'s > 18,000 km range as the majority of recordings came after Pettibone's 1991 re-description. Before Pettibone's re-description, *G. caeciliae* was known from the Eastern Atlantic (Fauvel 1913; Hartmann-Schroder 1985) and the Indian Ocean (Stock, 1986). Pettibone (1991) expanded the range to the Western Atlantic and the Caribbean. The remaining records (60%) have all been in the last 15 years and did not expand the range any further (Eckelbarger et al., 2005; Simpson and Watling 2011; Britayev et al., 2014; Tu et al., 2015; Macpherson et al., 2016; Serpetti et al., 2017). Pettibone's more detailed description would have theoretically allowed for a more precise identification and this, along with increased exploration, would explain the subsequent increase in recordings.

The taxonomic description of *G. caeciliae* has fallen into some of the known problems related to marine annelid descriptions: poor early descriptions; composite generic re-descriptions based on two or more geographically distant specimens; and an assumption of wide variation of characters within species, discussed in Hutchings and Kupriyanova (2018). Fauvel's 1913 description was based on two specimens from the Eastern Atlantic. When the species was re-described by Pettibone (1991) the non-type specimens examined and illustrated showed two different morphologies from either side of the Atlantic (Pettibone 1991, Figs. 12, 13, 14); this expanded the species range. However, the written description was a composite, making no mention of the morphological differences observed.

Given the potential that the descriptive taxonomic history based on morphology for *G. caeciliae* may not represent the true taxonomy, the aims of this study were: (i) to utilize modern molecular techniques to analyse the genetic variation/divergence in *G. caeciliae* collected from both the eastern and western basins of the Atlantic; and (ii) to carry out detailed morphological analysis, in tandem with molecular analysis, to determine if morphological characters could define any new species boundaries found. This study will add to the few wide-scale morphological and genetic investigations into deep-sea commensal marine annelids (e.g., Hatch et al., 2020; Lindgren et al., 2019). The results will increase the knowledge of deep-sea marine annelids and contribute to a better understanding of biodiversity patterns and biogeography of deep-sea fauna.

2. Methods

2.1. Specimen collection

A total of 82 specimens of *Gorgoniapolynoe* were examined. Sample collection was undertaken using ROV *Isis,* deployed from the *RRS James Cook* during the JC094 cruise in October/November 2013. Sampling locations were all between 05°N and 15°N in the central Equatorial Atlantic (Fig. 1; Table 1), on either side of the Mid-Atlantic Ridge, with the seamounts Vayda and Vema being in the western basin and Carter and Knipovich in the eastern basin. The sampling depths ranged from 600 to 2340 m. All worms were found in association with deep-sea octocorals from the families Acanthogorgiidae, Primnoidae and Coralliidae (Order Alcyonacea). The specimens were removed from tunnels within the coral tissue, with multiple individuals recovered from each coral. Once removed, worms were preserved in 70% ethanol and stored at −20 °C.

In addition, all the specimens examined by Pettibone for her 1991 re-description, which are part of the Smithsonian Institute's National Museum of Natural History collection, were also examined here. These specimens included Fauvel's original type material (USNM 80098) and a specimen from the type locality (USNM 133356).

Additionally, a specimen identified as *Harmothoe* cf. *bathydomus* found in association with an unidentified holothurian was collected at 1,012 m at the Cantabrian Sea (43°54.449′N, 6°15.494′W) in June 2017. The specimen was collected on board the B/O *Ángeles Alvariño* using a Beam trawl as part of the SponGES project. The polynoid was preserved in 96% ethanol and stored at −20 °C.

2.2. DNA extraction, amplification and sequencing

DNA was extracted from 82 specimens, using approximately 20 segments from the posterior of the body. DNA extraction was done using a DNeasy® Blood and Tissue kit (QIAGEN, Germany), following the manufacturer's protocol except for the final elution stage, where a final elution in 75 μL of Buffer AE was used.

The Folmer region (Folmer et al., 1994) of the mitochondrial Cytochrome *c* oxidase subunit I (*COI*) gene was amplified for these 82 specimens. These specimens represented individuals from each location and from multiple hosts (Table 1). Additionally, a fragment of the ribosomal mitochondrial gene 16S rDNA (*16S*) and the nuclear ribosomal genes 18S rDNA (*18S*) and 28S rDNA (*28S*) were amplified for five specimens (Table 1). These five specimens were selected based on genetic divergence inferred from analysis of the *COI* data and from features identified during morphological analyses. PCR protocols and primers are presented in Table 2 and the PCR profiles used were: *COI* [95 °C/5min – (95 °C/1min - 58 °C/1min - 72 °C/1min) x 38 cycles - 72 °C/10min]; *16S* [94 °C/5min – (94 °C/1min - 58 °C/45sec - 68 °C/45 s) x 38 cycles - 68 °C/10min]; *18S* [94 °C/5min – (94 °C/1min - 52 °C/1min - 72 °C/1min) x 38 cycles - 72 °C/10min]; *28S* a/Rd5b and C1/C2
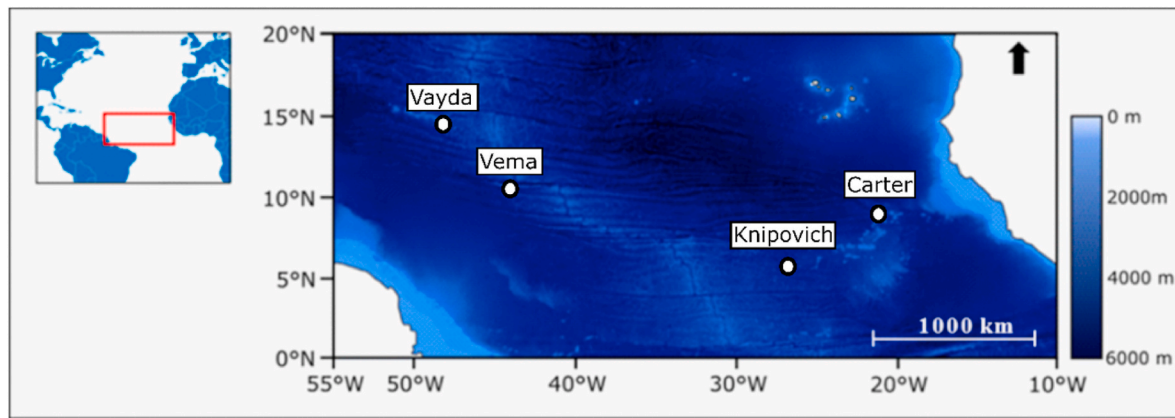
Fig. 1. Map of the study area with the locations of the four seamounts where the sampling was undertaken. See details about seamounts in Table 1.

Table 1

Summary of specimens *Gorgoniapolynoe* whose morphology was examined and for which *COI* marker was amplified, as well as specimens, including *G. caeciliae* type specimen, from National Museum of Natural History (USNM) and the additional *COI* markers sourced from GenBank. Parent ID of host corals, coral host identification, sampling depth, coordinates, specimen numbers (prefix) and number of individuals, are also indicated. *Indicates that one individual was also sequenced for 16S, 18S and 28S; [+]indicates that one individual was used for SEM, [#] indicates that one individual was used for histological analysis.

Specimens from Equatorial Atlantic used in morphological and molecular analysis

Seamount/Parent coral ID no.	Coral host	Depth (m)	Lat	Long	ID prefix	N
Gorgoniapolynoe caeciliae **MOTU 1**						
Vayda						
0096	*Corallium* sp.	1416	14° 51′N	48° 14′W	1819[#], 1851, 1879	11
1470	*Corallium* sp.	1622	14° 51′N	48° 15′W	2191[+], 2194*[+]	6
Vema						
0091	*Corallium* sp.	2190	10°46′N	44°36′W	1743*, 1771	3
0515	*Acanthogorgia* sp.	593	10° 42′N	44° 25′W	1714*, 1715	7
Gorgoniapolynoe caeciliae **MOTU**						
0091	*Corallium* sp.	2190	10°46′N	44°36′W	1743*, 1771[+]	6
Gorgoniapolynoe pseudocaeciliae **sp. nov.**						
Vayda						
0098	*Corallium* sp.	772	14°53′N	48°9′W	2029, 2030, 2031	3
1454	*Corallium* sp.	710	14°53′N	48°9′W	2054, 2086, 2087	4
Knipovich						
0083	*Corallium* sp.	1445	5°36′N	26°57′W	1217*, 1238, 1260	14
Carter						
0502	*Candidella* sp.	1783	9°12′N	21°17′W	0551	1
0024	*Corallium* sp.	1364	9°12′N	21°18′W	0602*[+#]	7
0061	*Corallium* sp.	2343	9°10′N	21°16′W	0680, 0716	16
0063	Primnoidae sp.	1364	9°12′N	21°18′W	0745	2
0064	*Corallium* sp.	1367	9°12′N	21°18′W	0671	2

Gorgoniapolynoe caeciliae specimens from USNM						
Specimen number	**Coral host**	**Depth (m)**	**Lat**	**Long**	**Location**	
USNM 80098 (Syntype)	*Pleurocorallium johnsoni*	1241	45°05′N	9°54′W	Gulf of Gascony	
USNM 21123	*Candidella imbricata*	512	13°34′N	61°03′W	St. Vincent, Lesser Antilles	
USNM 80091	*Candidella imbricata*	512	13°34′N	61°03′W	St. Vincent, Lesser Antilles	
USNM 133357	*Corallium niobe*	677	27°06′N	79°32′W	Straits of Florida	
USNM 80090	*Acanthogorgia aspera*	805	30°44′N	79°26′W	Off Georgia	
USNM 133356	*Corallium niobe*	1170	40°33′N	9°26′W	Off Portugal	

Note on USNM 133356: This specimen has been redetermined to be *Gorgoniapolynoe pseudocaeciliae* sp. nov. and should now be considered the holotype.

Additional *Gorgoniapolynoe COI* markers from South Indian Ocean, sourced from GenBank

Species	Coral host	Depth (m)	Lat	Long	Voucher	
Gorgoniapolynoe 'Indian Ocean' 1	*Narella* sp.	1360	41°20′S	42°55′E	NSJC66_104_1	
Gorgoniapolynoe 'Indian Ocean' 2	*Candidella imbricata*	1021	38°29′S	46°45′E	NSJC66_804_2	
Gorgoniapolynoe 'Indian Ocean' 3	*Acanthogorgia* sp.	784	32°41′S	57°17′E	NSJC66_4277_1	
Gorgoniapolynoe corralophila 1	Stylasteridae sp.	1357	41°20′S	42°55′E	NSJC66_133_S001	
Gorgoniapolynoe corralophila 2	Stylasteridae sp.	562	38°27′S	46°45′E	NSJC66_3219_S001	
Gorgoniapolynoe corralophila 3	Stylasteridae sp.	1340	37°56′S	50°27′E	NSJC66_3559_1	
Gorgoniapolynoe corralophila 4	Stylasteridae sp.	894	32°42′S	57°17′E	NSJC66_4279_S001	

[94 °C/5min – (94 °C/1min - 55 °C/1min - 72 °C/1min) x 30 cycles]; and *28S* F63.2/PO28R4 [95 °C/5min – (95 °C/30 s - 55 °C/30 s - 72 °C/1.5 min) x 30 cycles - 72 °C/10min].

All markers were amplified using 10.5 μL of VWR Red Taq DNA Polymerase 1.1x Master Mix (VWR International bvba/sprl, Belgium), 0.5 μL of the forward and reverse primers and 1 μL of DNA template. GelRed® (Biotium, USA) was used to stain the PCR products, which were visualised using 1.5% agarose gel electrophoresis. The PCR

Table 2
Primer pairs used for PCR and sequencing.

Primer	Sequence 5′-3′	Reference
COI		
LCO 1490	GGTCAACAAATCATAAAGATATTGG	Folmer et al. (1994)
HCO 2198	TAAACTTCAGGGTGACCAAAAAATCA	Folmer et al. (1994)
16S		
arL	CGCCTGTTTATCAAAAACAT	Palumbi (1996)
brH	CCGGTCTGAACTCAGATCACGT	Palumbi (1996)
18S		
1F	TACCTGGTTGATCCTGCCAGTAG	Giribet et al. (1996)
5R	CTTGGCAAATGCTTTCGC	Giribet et al. (1996)
4F	CCAGCAGCCGCGCTAATTC	Giribet et al. (1996)
7R	GCAAATAACAGGTCTGTGATGCCC	Giribet et al. (1996)
a2.0	ATGGTTGCAAAGCTGAAAC	Whiting et al. (1997)
9R	GATCCTTCCGCAGGTTCACCTAC	Giribet et al. (1996)
28S		
a	GACCCGTCTTGAAACACGGA	Whiting et al. (1997)
rD5b	CCACAGCGCCAGTTCTGCTTAC	Whiting (2002)
C1	CCTGGTTAGTTTCTTTTCCTCCGCT	Vän Le et al. (1993)
C2	TGAACTCTCTCTTCAAAGTTCTTTTC	Vän Le et al. (1993)
F63.2	ACCCGCTGAAYTTAAGCATAT	Struck et al. (2006)
PO28R4	GTTCACCATCTTTCGGGTCCCAAC	Struck et al. (2006)

products were then purified and sequenced at the Natural History Museum's (NHMUK) London sequencing facility. Overlapping sequence fragments for each marker were cleaned, assembled and trimmed using the program Geneious v.10.1.3 (http://www.geneious.com, Kearse et al., 2012). All consensus sequences were run through BLAST (Altschul et al., 1990) to check for contamination.

2.3. Species delimitation analysis

COI samples included in this analysis are found in Table 1 and in Supplementary Material Table S1. *Antipathypolyeunoa* sp. (GenBank accession number KU738202, supplementary material, Table S2) was used as an outgroup. Sequences were aligned in Geneious using the inbuilt MAFFT v.7.309 program (Katoh and Standley, 2013) and Q–INS–I option. The best partition schemes (including codon positions for protein-coding genes) and associated substitution models under AICc criterion were evaluated with PartitionFinder (Lanfear et al., 2016), using the greedy algorithm (Lanfear et al., 2012).

Once aligned and trimmed, *COI* sequences were 666 base pairs (bp) long. The sequences were checked for stop codons manually using the translate function (DNA to protein) in MEGA-X 10.0.5 (Kumar et al., 2018). Phylogenetic analyses were carried out using the model-based approach of maximum likelihood (ML), implemented using RAxML v8.2.12 (Stamatakis, 2014). RAxML was run using the GTR + GAMMA + I for all partition schemes as determined by PartitionFinder. The multiple tree search consisted of 100 alternative runs and the multiparametric bootstrap analysis had 1000 iterations.

Automatic Barcode Gap Discovery (ABGD, Puillandre et al., 2012) and a Bayesian implementation of the Poisson tree processes model (bPTP, Zhang et al., 2013) were used on the *COI* haplotype data to delimit species. ABGD was run online at https://bioinfo.mnhn.fr/abi /public/abgd/abgdweb.html, using the aligned *COI* sequences as the input. The program relies on the inclusion of the priors, P_{max} and P_{min}, where *P* is the divergence of intraspecific diversity. P_{min} was set at 0.001 and P_{max} at 0.37. These values were based on the range of intraspecific distances calculated for Polychaeta as a whole (Kvist, 2016). Twenty steps were run with a relative gap width (X) of 1.5. The number of bins for distance distribution was set to 50. Kimura (K80) model with TS/TV = 2 was used to calculate distance.

The bPTP model was run online at https://species.h-its.org/. The input file was the resulting tree from the *COI* RAxML analysis, converted into Newick format in Figtree v1.4.3 (Rambaut and Drummond, 2012). A haplotype data file was used to remove identical sequences, and only specimens collected for this study and the sequences identified as

G. caeciliae from GenBank, were used for the bPTP model. The number of MCMC generations was set at 500,000, with a thinning of 100 and a burn-in of 0.25. The outgroup was removed during this analysis. The mean distance between the resulting species was calculated using MEGA-X 10.0.5 (Kumar et al., 2018)

2.4. Phylogenetic analysis

Phylogenetic analyses were conducted using five specimens of *Gorgoniapolynoe* from our dataset and a selection of sequences from individuals of *Gorgoniapolynoe* found online at the NCBI within the family Polynoidae (Supplementary material, Table S1). The five specimens from our dataset were selected to represent the genetic variation seen in the *COI* tree constructed for species delimitation. Additional material identified as *Harmothoe* cf. *bathydomus* from the Cantabrian Sea was also sequenced and included in the analysis. All alignments were manually trimmed and concatenated in Geneious. Gblocks v.0.91b (Castresana, 2000) was run separately for the alignments of the non-coding genes (*16S*, *18S* and *28S*). Gblocks was used to clean poorly aligned positions and to eliminate divergent regions, following previous papers for comparative purposes (Gonzalez et al. 2018; Serpetti et al. 2017; Taboada et al. 2020a). Given that the data set has individuals belonging to different families within the order Aphroditiformia, without the use of Gblocks both methods did not return meaningful trees. The "minimum length of a block" was set at 5, "allowed gap positions" was set at "with half", "maximum number of contiguous non-conserved positions" was set at 10 and finally the "minimum number of sequences for a flanked position" was set at $\frac{2}{n} + 1$, where n = total number of sequences. Once each marker was aligned, trimmed and run through Gblocks, they were concatenated, resulting in a 3,553 bp length alignment (*16S* = 438 bp, *18S* = 1,648 bp, *28S* = 900 bp and *COI* = 567 bp).

RAxML only allows for a single model of rate heterogeneity in partitioned analysis, so GTR + I + G was chosen as it was suggested for four out of the six partitions and had a low AICc score for the remaining two partitions. The other parameters were set as previously described for *COI*. In MrBayes, the Monte Carlo Markov Chains (MCMC) were run for ten million generations, with trees sampled every thousand generations using the following evolutionary models for each partition, *16S*, *18S*, *28S* and *COI* (3rd position) = GTR + I + G, *COI* (1st position) = HKY + G and *COI* (2nd position) = GTR. Across the partitions, the parameters of substitution rates, nucleotide frequencies, invariant-sites proportion and gamma shape were all unlinked. Burn-in was set at 25%. Tracer v1.7.1 (Rambaut et al., 2018) was used to check for convergence. Analysis was stopped once the standard deviation of split frequencies was <0.01, the potential scale reduction factor PSRF was around 1.00, the effective sample sizes were >200 and the trace plot had the appearance of a "hairy caterpillar".

2.5. Demographic analyses

The *COI* alignment of *Gorgoniapolynoe* from the central Equatorial Atlantic was used to construct unrooted haplotype networks with the program *PopART* (Leigh and Bryant, 2015) by implementing the Templeton, Crandall and Sing (TCS) method (Templeton et al., 1992; Bandelt et al., 1994).

The levels of DNA polymorphism, polymorphic and parsimony-informative sites were calculated for each sampling region and lineage using DNASP vs. 5.10.1 (Rozas et al., 2017) and included the number of haplotypes (*H*), private haplotypes (*Hp*), haplotype diversity (*Hd*) and nucleotide diversity (*π*).

An analysis of molecular variance (AMOVA) was used to determine differentiation between areas and hosts for each of the species identified in the morphological and phylogenetic analyses. AMOVA was run using Arlequin v3.5.2.2 (Excoffier and Lischer, 2010) under the hierarchy of location (seamount) > population (host). *F*-statistics were utilised to

estimate the proportion of variability found between locations (F_{ct}), among populations within locations (F_{sc}) and within populations (F_{st}). Data was grouped into depth bins (500–1000 m, 1000–1500 m, 1500–2000 m and >2000 m) and an AMOVA was also run to determine if depth was a factor in any genetic variation, under the hierarchy of depth > host.

2.6. Morphological analysis

The macroscopic morphological characters of all collected specimens were examined using a Leica MZ6 stereomicroscope (Leica Microsystems, Germany). Parapodia and elytra were removed from selected specimens for further examination under an Olympus BX43 compound microscope (Olympus Corporation, Japan). Specimens were photographed using an Olympus UC50 camera and the cellSens Standard interface (Olympus Corporation, Japan) for both microscopes.

The syntype of *Gorgoniapolynoe caeciliae* (USNM 80098), designated by Fauvel in 1913, was reexamined, as well as all the material examined by Pettibone (1991; Table 1) which included specimen (USNM 133356) from the type locality. All literature on *G. caeciliae*, from the original description by Fauvel (1913) to the most recent work by Britayev et al. (2014) was used as references throughout the morphological analysis.

Four specimens were selected for analysis using a scanning electron microscope (SEM) (Table 1). In order to assess if any genetic variability corresponded with differences in morphology, specimens were chosen based on their positioning within the *COI* tree. Specimens were dehydrated in an ascending ethanol series from 70 to 100%, critical-point-dried in a Balzers CPD-030 dryer (Bal-Tec AG, Liechtenstein), mounted on stubs and coated with gold (20 nm). Imaging was performed using Zeiss Ultra Plus Field Emission SEM (Zeiss Group, German) in the NHMUK imaging facilities.

2.7. Histological preparations

Two specimens were selected for histological analysis. One specimen was selected from each of the two species (*G. cf caeciliae* and *G. pseudocaeciliae* sp. nov.) observed as a result of the morphological and phylogenetic analyses, with the criteria for selection being the presence of a pair of modified first elytra and the subsequent smaller unmodified second pair. The anterior portion of each two specimens (prostomium and following five to six segments) was dehydrated in an increasing ethanol series (50%, 70%, 96% and 100%), cleared in xylene and embedded in melted paraffin, then sliced into 5 μm sections using an Autocut Reichert-Jung microtome 2040 (R. Jung GmbH, Nubloch, Germany), stained with haematoxylin-eosin and mounted with DPX. Prepared slides were investigated using Olympus BX43 compound microscope (Olympus Corporation, Japan) and imaged using an Olympus UC50 camera and the cellSens Standard interface (Olympus Corporation, Japan).

3. Results

3.1. Molecular analysis

3.1.1. Species delimitation

Both the ABGD and bPTP (Supplementary Material Fig. S1) analyses supported *Gorgoniapolynoe pseudocaeciliae* sp. nov. as a single species distinct from all other groups in the dataset. ABGD delimited the group as a single species for all values of intraspecific divergence (*P*) up to 0.0307 (3.07%) (Supplementary Material Fig. S2). *Gorgoniapolynoe pseudocaeciliae* sp. nov could also be distinguished from *G.* cf. *caeciliae* using morphological characters. *Gorgoniapolynoe pseudocaeciliae* sp. nov has a smaller modified area on the first elytra, a more pronounced and digiform neuropodial postsetal lobe and none of the notochaeta have spinous pockets (see section 3.2.)

An intraspecific divergence range of *P* = 0.001–0.0225 (0.1–2.25%)

in ABGD returned two apparent molecular operational taxonomic units (MOTUs) within *G.* cf. *caeciliae*, despite no apparent morphological difference (supplementary material, Fig. S2). The bPTP model also inferred the presence of two species within *G.* cf. *caeciliae* (supplementary material, Fig. S1) At *P* = 3.07% ABGD no longer delimited *G.* cf. *caeciliae* into two MOTUs, while at *P* = 4.19% ABGD returned the complete data set as a single species (supplementary material, Fig. S2).

Both ABGD and bPTP infer that *Gorgoniapolynoe caeciliae* from the Indian Ocean obtained from GenBank (Serpetti et al., 2017) are a distinct species. Henceforth within this text, they will be referred to as *Gorgoniapolynoe* 'Indian Ocean'. The ABGD model delimited all individuals labelled as *G. corralophila* as a single distinct species.

The mean intraspecific distance between the different delimited species ranged from 7 to 15%, with the smallest distance being between the two MOTUs in *G.* cf. *caeciliae* (supplementary material, Table S2).

3.1.2. Haplotype network analyses

A total of 26 haplotypes were recovered out of the 33 individuals identified as *Gorgoniapolynoe* cf. *caeciliae* (Fig. 2). The haplotype network of the larger MOTU in *G.* cf. *caeciliae* (Unit 1) recovered a diffuse topology, with 22 haplotypes from 27 individuals. The haplotype diversity (Hd) in *G.* cf. *caeciliae* Unit 1 was 0.98 ± 0.0003 and all the haplotypes, except one, were private (Table 3). Out of the 22 Unit 1 haplotypes, only one was recovered from both seamounts. The six specimens of the smaller *G.* cf. *caeciliae* MOTU (Unit 2) had four haplotypes (Fig. 2), with a Hd of 0.867 ± 0.129, all of which were found on a single host from Vema. The nucleotide diversity (π) for *G.* cf. *caeciliae* Unit 1 and Unit 2, was 0.01512 ± 0.00189 and 0.00494 ± 0.00119, respectively (Table 3) and the number of mutations separating them was 17.

For *Gorgoniapolynoe pseudocaeciliae* sp. nov. the haplotype network topology was also diffuse, returning 22 haplotypes out of the 49 individuals (Fig. 2), with a Hd = 0.929 ± 0.02. There were 16 private haplotypes. The nucleotide diversity was 0.00977 ± 0.000001 (Table 3). Three haplotypes were shared across all three seamounts from which *G. pseudocaeciliae* were collected, Carter and Knipovich in the east and Vayda in the west. These three shared haplotypes were found across the entire sampled depth range, ≈700–2,340 m (Fig. 2). There were three other haplotypes shared between seamounts, but these were only observed for the East Atlantic seamounts, separated by approximately 600 km and found between 1,360 and 2,340 m.

3.1.3. AMOVA

AMOVA results for *G. pseudocaeciliae* sp. nov. showed no significant variation between seamounts or between coral hosts. There was significant variation on individual hosts (Table 4). Depth was found not to be a significant factor to genetic variation in *G. pseudocaeciliae* sp. nov. (Table 4). The results for *G.* cf. *caeciliae* Unit 1 also showed no significant variation between seamounts, between hosts, or between depth bins, with the only significant variation found to be on individual host corals. No analysis was run on *Gorgoniapolynoe* cf. *caeciliae* Unit 2, as it was only found at Vema on a single host.

3.1.4. Phylogenetic analyses

Polynoidae was recovered as monophyletic although only with high support from the Bayesian Inference analysis, Posterior Probability (PP) = 0.9, Bootstrap value (BS) = 66 (Fig. 3). The subfamily Polynoinae was not returned as monophyletic due to the inferred positions of *Paradyte crinoidicola* (Potts, 1910) and *Paralepidonotus ampulliferus* (Grube, 1878), as well as the positioning of the Lepidonotinae *Lepidonotus sublevis* Verrill, 1873.

Members of the genus *Gorgoniapolynoe* were all recovered in a fully supported monophyletic clade (PP = 1.0, BS = 100; Fig. 3). The two individuals identified as *Gorgoniapolynoe pseudocaeciliae* sp. nov. (JC094_602 × 007 and JC094_1217 × 006) grouped together. The three *Gorgoniapolynoe* 'Indian Ocean' specimens were recovered closest to
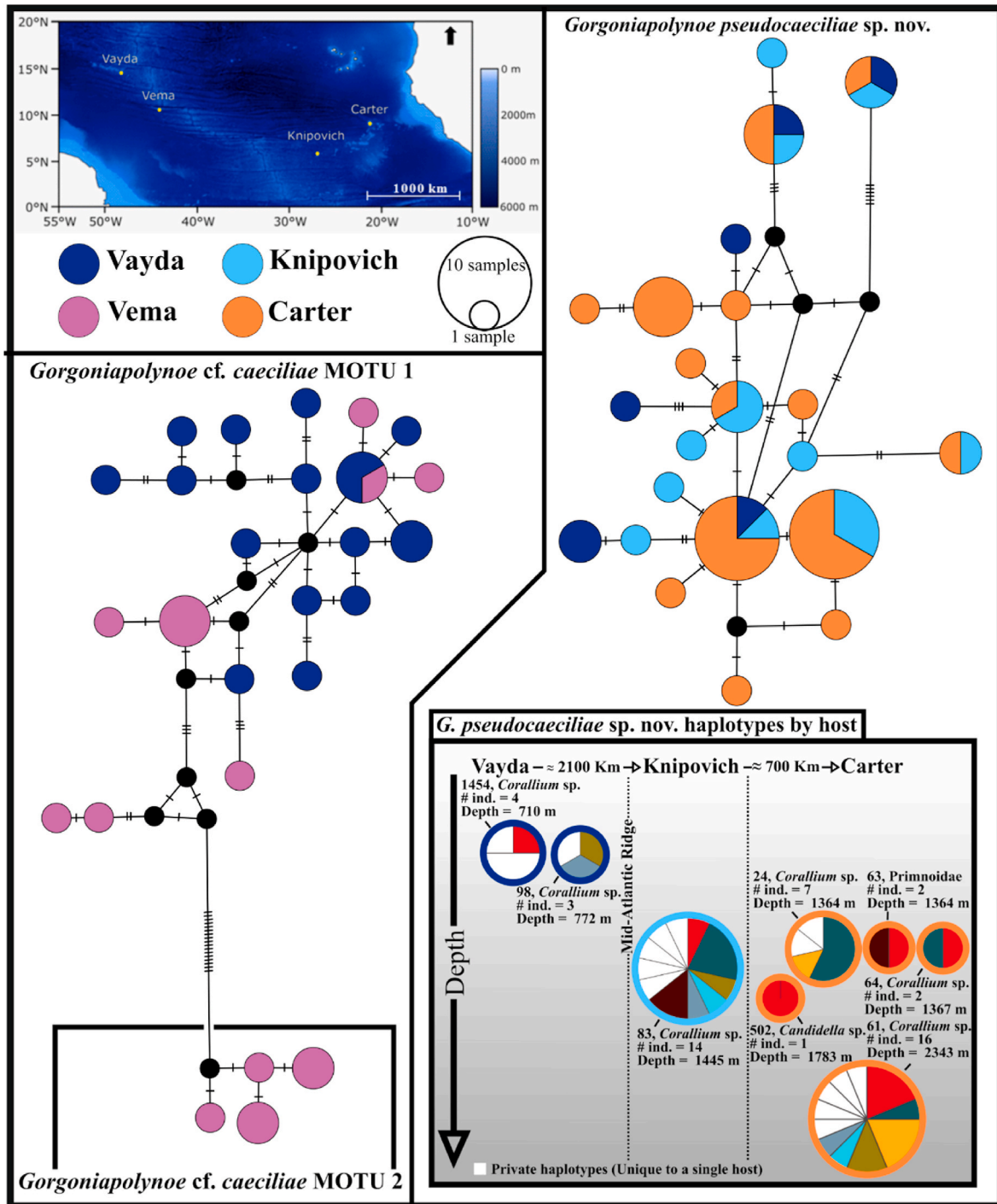
Fig. 2. *COI* haplotype networks from *Gorgoniapolynoe caeciliae* MOTU 1, MOTU2 and *G. pseudocaeciliae* sp. nov. There are 27 individuals in *G. caeciliae* MOTU 1, 6 in *G. caeciliae* MOTU2 and 29 individuals in *G. pseudocaeciliae* sp. nov. Dashes represent mutation steps. Missing inferred haplotypes are in black. Also shown are the shared haplotypes for *G. pseudocaeciliae* by host, the white segments represent private haplotypes, i.e., haplotypes which are exclusive to a single host. **(Colour should be used)**.

G. pseudocaeciliae sp. nov. (PP = 1.0, BS = 86), followed by *G. corralophila* (PP = 1.0, BS = 82). The two *Gorgoniapolynoe* cf. *caeciliae* MOTU 1 (JC094_1714 × 007 and JC094_2194 × 006) and *Gorgoniapolynoe* cf. *caeciliae* MOTU 2 (JC094_1743 × 003) formed a sister group to the rest of the *Gorgoniapolynoe* specimens (PP = 1.0, BS = 100).

3.2. Taxonomic descriptions

Family Polynoidae Kinberg, 1856.

Genus *Gorgoniapolynoe* Pettibone, 1991.
Gorgoniapolynoe cf. caeciliae.
Fig. 4.
Fauvel (1913):24, Fig. 7 A–D. 1914:69, pl. 4: Figs. 1–6, 18–19. 1923:82, Fig. 31a-h.
Belloc, 1953:4.
Pettibone (1991): Fig. 14.
Britayev et al. (2014):34, Fig. 5c–h, 8, 9, 10.

Table 3
Nucleotide and haplotype information for each *Gorgoniapolynoe* species from this study. Data is presented for all locations combined and for each individual seamount. N = number of individuals, Pi = nucleotide diversity, h = number of haplotypes, Hd = Haplotype diversity, Ph = Private haplotypes, %Ph = percentage of haplotypes which are private. *private haplotypes for combined seamounts refer to haplotypes found on a single host, Ph of individual seamounts refers to haplotypes unique to that seamount. SD = Standard deviation [+] *Gorgoniapolynoe* cf. *caeciliae* MOTU 2 was collected from a single host coral on Vema so has no private haplotypes.

	N	Pi	h	Hd ±SD	Ph	% Ph
Gorgoniapolynoe pseudocaeciliae sp. nov.						
Combined Seamounts	49	0.00977 ± 0.0000012	22	0.929 ± 0.02	16*	73
Vayda	7	0.01566 ± 0.00289	6	0.952 ± 0.096	3	50
Knipovich	14	0.00897 ± 0.00192	11	0.956 ± 0.045	5	45
Carter	28	0.00735 ± 0.00112	14	0.902 ± 0.035	7	50
Gorgoniapolynoe cf. *caeciliae* MOTU 1						
Combined Seamounts	27	0.01512 ± 0.00189	22	0.980 ± 0.017	20*	91
Vayda	17	0.01200 ± 0.00144	15	0.985 ± 0.025	14	93
Vema	10	0.01602 ± 0.00289	8	0.933 ± 0.007	6	75
Gorgoniapolynoe cf. *caeciliae* MOTU 2						
Vema	6	0.00494 ± 0.00119	4	0.867 ± 0.129	NA[+]	NA[+]

3.2.1. Material examined

Eastern North Atlantic: Syntype of *Gorgoniapolynoe caeciliae,* Prince de Monaco, station 2743, 45°05′N, 9°54′W, Gulf of Gascony, 1241 m, July 27, 1908, on *Pleurocorallium johnsoni,* (USNM 80098).

Western North Atlantic Ocean: *USS Albatross,* station 2753, 13°34′N, 61°03′W, off St. Vincent, Lesser Antilles, 512 m, Dec 4, 1886, on *Candidella imbricata,* two specimens, removed by F. M. Bayer (USNM 21123) and eight specimens, removed by M. Pettibone (USNM 80091). R/V Gerda cruise 6333, station G170, 27°06′N, 79°32′W, Straits of Florida, east of St. Lucie Inlet, 659–677 m, June 29, 1963, on holotype of *Corallium niobe,* three specimens, removed by F. M. Bayer (USNM 133357). *USS Albatross*, station 2415, 30°44′N, 79°26′W, Off Georgia, 805 m, April 1, 1885, on *Acanthogorgia aspera,* two specimens, removed by F. M. Bayer (USNM 80090).

Central West Atlantic: *RRS James Cook*, JC094 station 41, 10° 42′N, 44° 25′W, Vema Seamount, 593 m, Nov 12, 2013, on *Acanthogorgia* sp., seven specimens (JR094_1714 × 001 to 002, JR094_1714 × 006 to 007, JR094_1715 × 001 to 003); *RRS James Cook*, JC094 station 42, 10°46′N, 44°36′W, Vema Seamount, 2190 m, Nov 13, 2013, on *Corallium* sp., nine specimens (JR094_1771 × 001 to 005, JR094_1771 × 004 (SEM stub), JR094_1743 × 002 to 005). *RRS James Cook*, JC094 station 45, 14° 51′N, 48° 14′W, Vayda Seamount, 1416m, Nov 17, 2013, on *Corallium* sp., 11 specimens (JC094_1819 × 001, JC094_1819 × 002 (used for histological analysis), JC094_1851X001 to 005, JC094_1879X002 to 004, JC094_1879X008). *RRS James Cook*, JC094 station 49, 14° 51′N, 48° 15′W, Vayda Seamount, 1622 m, Nov 21, 2013, on *Corallium* sp., six specimens (JC094_2191 × 005 (SEM stub), JC094_2194 × 001 to 003, JC094_2194 × 003 (SEM stub), JC094_2194 × 006 to 007).

All specimens examined from Vema and Vayda seamounts are catalogued at the NHM London.

3.2.2. Description

Body ranging in length from 11 to 22 mm, 2–2.7 mm wide (inclusive of chaetae), with up to 52 segments. Body almost cylindrical anteriorly, becoming progressively more dorso-ventrally flattened from segments 15–20 (Fig. 4A). Prostomium bilobed, with rounded lobes without cephalic peaks, wider than long. Two pairs of large eyes, with anterior pair

Table 4
The results of analysis of molecular variance (AMOVA) on the *COI* data for *Gorgoniapolynoe* from the Equatorial North Atlantic. Species were determined using morphology and species delimitation models ABGD and bPTP. Depth bins were 500–1000 m, 1000–1500 m, 1500–2000 m and >2000 m. * marks significant variation ($p < 0.05$).

Location					
Source of variation	d.f.	Sum of squares	% of variance	*F*-statistics	*P*
G. pseudocaeciliae sp. nov.					
Between seamounts	2	83.872	0.67580	$F_{CT} = 0.05545$	0.26026+- 0.00335
Between hosts within a location	5	97.759	2.64236	$F_{SC} = 0.22954$	0.13151+- 0.00229
On individual hosts	41	363.634	8.86912	$F_{ST} = 0.27226$	0.01768+- 0.00097*
G. cf. caeciliae MOTU 1					
Between seamounts	1	82.057	2.73388	$F_{CT} = 0.08762$	0.66557+- 0.00328
Between hosts within a location	2	88.382	3.15591	$F_{SC} = 0.11086$	0.13985+- 0.00256
On individual hosts	23	582.154	25.31103	$F_{ST} = 0.18877$	0.02063+- 0.00096*
Depth					
Source of variation	d.f.	Sum of squares	% of variance	*F*-statistics	*P*
G. pseudocaeciliae sp. nov.					
Between different depth bins	3	6.952	−2.59	$F_{CT} = -0.02588$	0.24823+- 0.00277
Between hosts in the same depth bin	4	10.699	4.88	$F_{SC} = 0.04760$	0.18749+- 0.00284
On individual hosts	41	89.247	97.70	$F_{ST} = 0.02296$	0.24823+- 0.00277
G. cf. caeciliae MOTU 1					
Between different depth bins	2	150.310	23.52	$F_{CT} = 0.23518$	0.49451+- 0.00344
Between hosts in the same depth bin	1	20.129	−2.07	$F_{SC} = -0.02708$	0.27989+- 0.00302
On individual hosts	23	582.154	78.55	$F_{ST} = 0.21446$	0.02073+- 0.00095*

generally larger. Median antenna long and tapering, attached to ceratophore in the notch between prostomium lobes. Lateral antennae subulate and approximately a third the length of the median antenna. Ceratophores of the lateral antennae robust and cylindrical, slightly wider in diameter than antennae, inserted lateroventrally, slightly separated from the median antenna. Two stout palps dorsoventrally to the proboscis, as long as the median antenna (Fig. 4A and B). Robust tentaculophores lateral to the prostomium on the achaetous first segment. A pair of dorsal and ventral tentacular cirri. Dorsal cirri as long/longer than the median antenna. Ventral pair slightly shorter than the dorsal pair. Segment 2 with the first pair of elytrophores and the first biramous parapodia. Subulate buccal cirri emerge from short cylindrical cirrophores on the anterior ventral surface of the neuropodia, of similar length to the dorsal tentacular cirri.

A total of 15 pairs of elytra on segments 2, 4, 5, 7, then every second segment until 23, after which on segments 26, 29 and 32. First pair of elytra, larger than the subsequent ones, covering the prostomium. A large bean-shaped transparent chitinous area covers over half the elytra area. Chitinous area contains scattered rounded microtubercles and more regularly spaced elongated, barrel-shaped macropapillae (Fig. 4B, C, D). Following smaller elytra oval with down-curved borders and with barrel-shaped macropapillae randomly and sparsely scattered across the dorsal surface. Area of the elytra above elytrophore darker in colour.
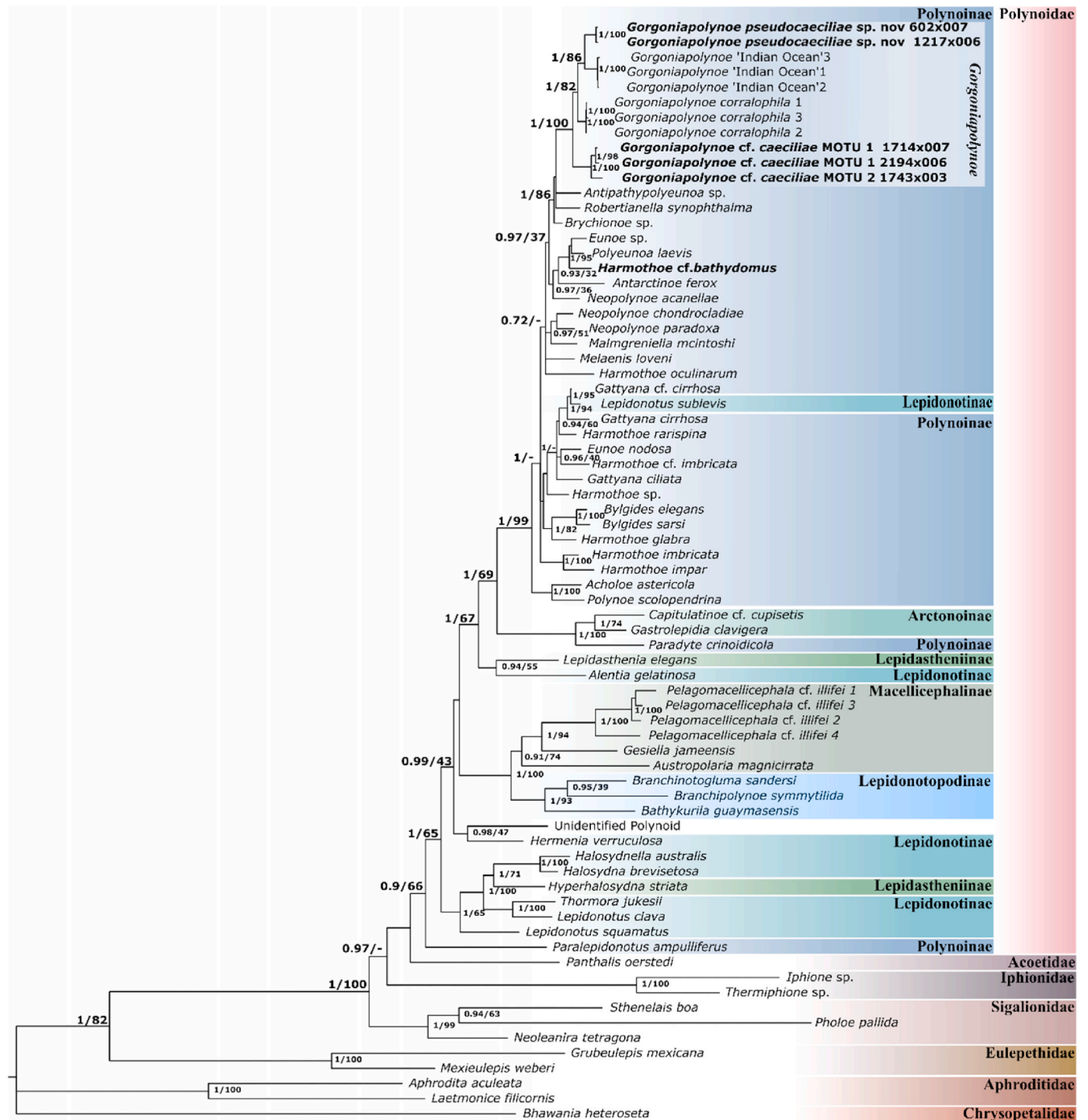
Fig. 3. Phylogenetic tree of Aphroditiformia, recovered from analysis of the concatenated sequences of *16S, 18S, 28S* and *COI*. The tree topology is based on Bayesian Inference analysis. Node labels are the posterior probability from BI analysis, followed by the bootstrap support from Maximum likelihood analysis. Families within Aphroditiformia and subfamilies within Polynoidae are colour coded. Individuals from the genus *Gorgoniapolynoe* are highlighted. All species in bold were sequenced for this study. See Supplementary Table S1 for NCBI accession numbers. **(Colour should be used).**

Very faint nerves present in elytra, only visible under microscope. Paired elytra do not touch leaving the mid-dorsum exposed. Emerging from tips of all macropapillae of all elytra are 3–4 cilia, that appear to be retractable wit yond the elytra boundary. Cilia have golf club-shaped structures at the distal end that are an artefact of preservation and are called "paddle cilia", AKA "discocilia" (Fig. 4F).

Dorsal cirri present on segments without elytra around three times as long as parapodia; sporadic clavate papillae present on proximal ends.

Cylindrical cirrophores along posterior side of notopodium. Starting on the third segment ventral cirri present on all segments. Base of ventral cirri slightly inflated before tapering, reach past the tip of neuropodium. From segment 10, bulbous, swollen area on base of ventral cirri causing them to project posteriorly. Transverse bands of short cilia present dorsally on random segments along the body. Posterior most segments without elytra have transverse ciliary bands with cilia over three times as long, more densely packed than is seen on any other segments (see
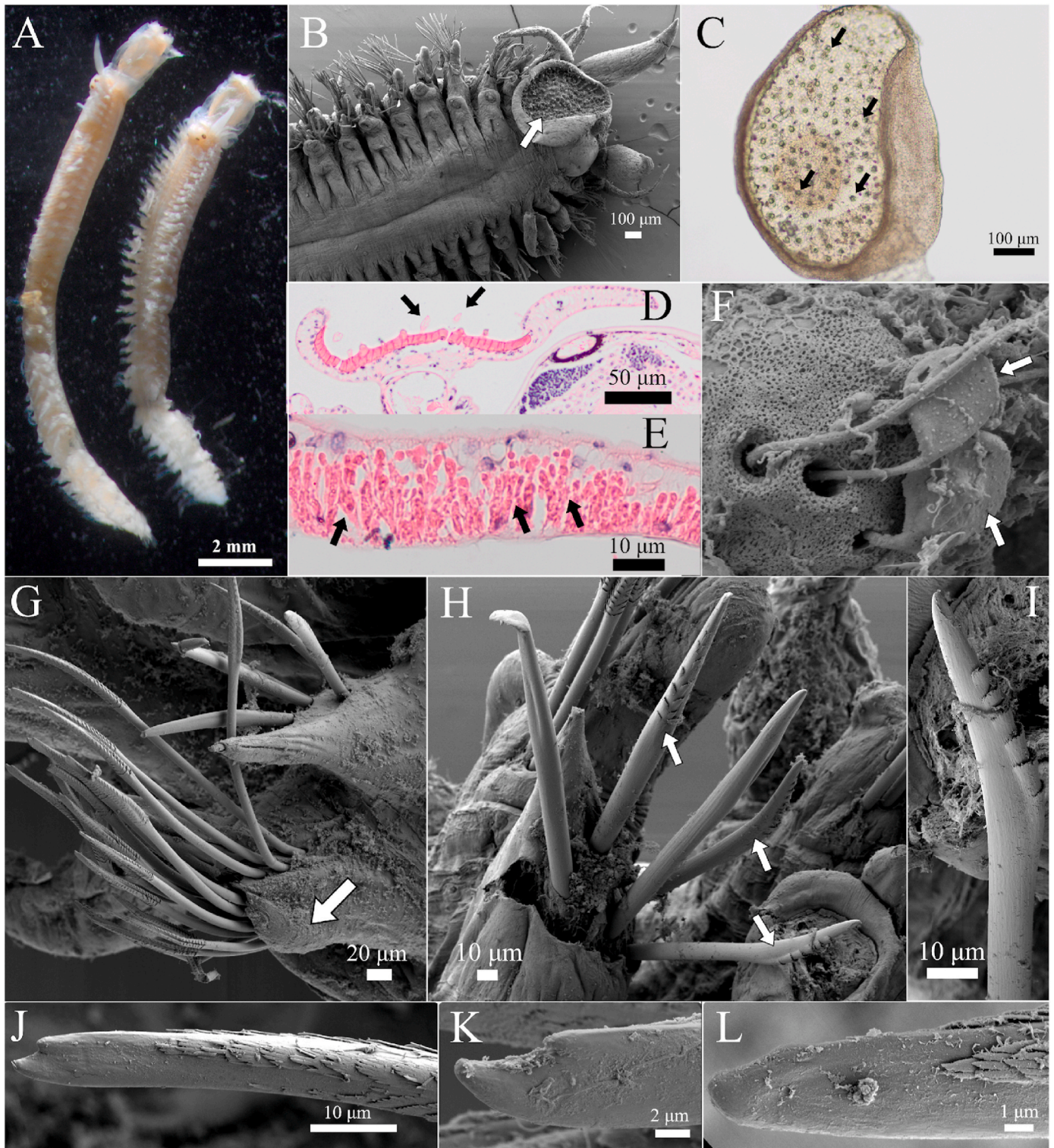
Fig. 4. Morphology of *Gorgoniapolynoe caeciliae* MOTU 1 and MOTU 2. **A)** Full body preserved specimens (USNM 21123). **B)** Anterior region of JC094_2194X003, showing the modified first elytra (arrow). **C)** The modified first eytra with the chitinous area. Arrows point out some of the macropapillae. **D)** Histological section of the modified first elytra of JC094_1819 × 002 showing the chitinous area, with papilla (arrows). **E)**. Photocyte-like cells concentrated around the elytrophore in posterior elytra (arrow). Same specimen as D. **F)** Newly observed cilium structures (arrows) emerging from the tips of a macropapillae in the chitinous area of the modified elytra of JC094_2194 × 003. Note flattened golf club head shaped structures at the distal end of the structures which are most likely "paddle cilia" **G)** Posterior side of 3rd parapodium of JC094_1771 × 004, showing the flattened, rounded neuropodial postsetal lobe (arrow). **H)** Two types of notochaeta on JC094_2194 × 003, the newly observed chaetae with alternating spinous pockets (arrows) and the smooth slightly curved chaetae. **I)** Detail of notochaeta with spinous pockets. **J)** Detail of tip of dorsal most neurochaetae. **K)** Detail of tip of mid-neurochaetae. **L)** Detail of tip of ventral most neurochaetae. J, K and L are all from the 3rd neuropodium on JC094_2194 × 003.

Fig. 5E and F for similar structures seen on *Gorgoniapolynoe pseudocae-ciliae* sp. nov.). Large, digitate nephridial papillae from segment six, posterior-ventrally positioned on the parapodium, becoming less prominent in posterior segments.

Parapodia biramous. Notopodium is a subconical acicular lobe. Neuropodium longer and wider with presetal and postsetal lobes. Neu-ropodial presetal lobe diagonally truncated, projecting dorsally. A shorter flattened postsetal lobe lays close to neurochaetae; rounded, projecting slightly ventrally in anterior segments so that it can just be seen when viewed from anterior (Fig. 4G). On posterior segments the postsetal lobe becomes reduced to a small bump roughly in line with the neuroacicula, no longer visible when viewed from the anterior. Reduc-tion in the size of postsetal lobe begins approximately a third of the way down the body and is at its most reduced by the final third of the body. Notochaetae number between 3 and 7 on the first 10–15 segments (Fig. 4H), reduced to 2–4 after that. Two types of notochaetae present on anterior segments: stout acicular and slightly curved chaeta, with the groove on outside of the curve (Fig. 4H), and also stout, acicular and curved but with alternating spinous pockets from the apex of the curve to the tip (Fig. 4H and I). Both types of notochaetae positioned anterior to the notopodium and longer than it. Neurochaetae number between 10 and 15, as stout as notochaetae. Last third becomes quill-like, with spinose rows on dorsal surface. All neurochaetae tips bidentate to varying degrees and change in form moving dorsal to ventral. Supra-acicular neurochaetae have a large blunt tooth with a smaller rounded secondary tooth (Fig. 4J). Two forms of infraacicular neurochaetae present: the set closest to the supraacicular neurochaetae with a large pointed tooth slightly hooked and a secondary smaller tooth slightly more distinct than those in supraacicular neurochaetae (Fig. 4K); the most ventral infraacicular neurochaetae have a large blunt rounded tooth with a highly reduced secondary tooth barely more than a bump (Fig. 4L).

Pygidium is a blunt cone, with a pair of anal cirri at the terminus. Bases of the anal cirri closely situated almost touching, positioned slightly dorsally on the pygidium. Anal cirri as long or slightly longer than the dorsal cirri. Anus ventral to the cirri, protruding slightly.

3.2.3. Histological examination

Histological sections reveal darker area of smaller elytra correspond to presence of cup-like cells, possible photocytes (Fig. 4E).

3.2.4. Remarks

The morphology of *G.* cf. *caeciliae* parapodia appears to match the parapodial syntypes of *Gorgoniapolynoe caeciliae* (USNM 80098), most notably in the shape and orientation of the postsetal lobe. The morphology of the rest of the body also matches that of Fauvel's original written description, although the description is extremely limited. It cannot be said with confidence that the specimens examined in this study are *G. caeciliae*.

The morphological characters of *G.* cf. *caeciliae* are the same as the specimens examined by Pettibone (1991) for her redescription of the species. The presence of 3–7 notochaetae on anterior segments, observed on the Equatorial Atlantic specimens, were not mentioned or illustrated in Pettibone (1991). On re-examination of USNM 21123 (two specimens), we observed 4–6 notochaetae on segments three, five, six, eight of one specimen and segments three, five and ten on the other. The newly observed notochaetae in *G. caeciliae* are similar in appearance to the notochaetae seen in *G. corralophila* (Day, 1960), however, in the latter species they are much larger and can be easily observed under low magnification. Additionally, the specimens USNM 80090, 80091 and 133357, all of which were examined by Pettibone for her description, agree with the morphological features observed for *G.* cf. *caeciliae.*

Gorgoniapolynoe cf. *caeciliae* contain morphologically identical but genetically diverged individuals, which may be a cryptic species. The analysis of the *COI* sequences revealed that six of the 43 individuals identified as *G.* cf. *caeciliae* were genetically distinct and were inferred to

be a separate species: *G.* cf. *caeciliae* Unit 1 and 2, under ABCD and bPTP models (see section 3.1.1.) As the number of specimens is so low, no morphological differences could be found and the uncertain taxonomic affinity of the specimens in the first place, we prefer to be conservative and stop short of dividing it into two species. It may be that *G.* cf. *cae-ciliae* has high intraspecific genetic variability, hence why we have referred to them as MOTUs.

Gorgoniapolynoe pseudocaeciliae sp. nov.
Fig. 5.

Material examined: Eastern North Atlantic: Syntype of *Gorgoniapoly-noe caeciliae,* Prince de Monaco, station 2743, 45°05′N, 9°54′W, Gulf of Gascony, 1241 m, July 27, 1908, on *Pleurocorallium johnsoni*, (USNM 80098). *RV Thalassa,* station Y405, 40°33′N, 9°26′W, Off Portugal, 1170 m, 1st Sept 1972, on *Corallium niobe*, identified by M. Grasshoff, from G. Hartmann-Schröder, one specimen (USNM 133356).

Central East Atlantic: *RRS James Cook*, JC094 station 07, 9°12′N, 21°17′W, Carter Seamount, 1783 m, Oct 22, 2013, on *Candidella* sp., one specimen (JC094_551_001). *RRS James Cook*, JC094 station 11, 9°10′N, 21°16′W, Carter Seamount, 2343 m, Oct 23, 2013, on *Corallium* sp., 16 specimens (JC094_680_001to 008, JC094_716_001 to 008). *RRS James Cook*, JC094 station 15, 9°12′N, 21°18′W, Carter Seamount, 1364 m, Oct 26, 2013, on Primnoidae, two specimens (JC094_745_001 to 002). *RRS James Cook*, JC094 station 15, 9°12′N, 21°18′W, Carter Seamount, 1366 m, Oct 26, 2013, on *Corallium* sp., 7 specimens (JC094_602_001, JC094_602_003 to 007, JC094_602_008 - SEM stub). *RRS James Cook*, JC094 station 15, 9°12′N, 21°18′W, Carter Seamount, 1366 m, Oct 26, 2013, on *Corallium* sp., two specimens (JC094_671_001 to 002).

Central East Atlantic: *RRS James Cook*, JC094 station 21, 5°36′N, 26°57′W, Knipovich Seamount, 1445 m, Oct 30, 2013, on *Corallium* sp., 14 specimens (JC094_1217_001 to 006, JC094_1238_002 to 007, JC094_1260_003 to 004).

Central West Atlantic: *RRS James Cook*, JC094 station 48, 14°53′N, 48°9′W, Vayda Seamount, 772 m, Nov 18, 2013, on *Corallium* sp., three specimens (JC094_2029_000, JC094_2030_000, JC094_2031). *RRS James Cook*, JC094 station 48, 14°53′N, 48°9′W, Vayda Seamount, 710 m, Nov 18, 2013, on *Corallium* sp., four specimens (JC094_2054_000, JC094_2086_001, JC094_2087_001 to 002).

Suggested holotype: USNM 133356, east Atlantic.

3.2.5. Description

Body ranging from 13 to 22 mm long, 2.5–3.2 mm wide (inclusive of chaetae), with 38–51 segments.

Body almost cylindrical anteriorly, becoming progressively more dorso-ventrally flattened after approximately segment 13 (Fig. 5A). Bilobed prostomium with rounded lobes without cephalic peaks. Pro-stomium wider than long. Two pairs of large eyes present, with the anterior-most pair generally larger. A median antenna present, long and tapering, attached to ceratophore in a notch between prostomium lobes. A pair of short subulate lateral antennae, approximately a third the length of the median antenna inserted lateroventrally. Ceratophores of the lateral antennae cylindrical and slightly wider than the antennae. Two stout palps lateral to the lateral antenna as long as the median antenna. Robust tentaculophores present lateral to the prostomium on the achaetous first segment. Pairs of dorsal and ventral tentacular cirri. Dorsal tentacular cirri as long as the median antenna, with the ventral tentacular cirri slightly shorter than dorsal ones. Segment 2 with the first pair of elytrophores, ventral buccal cirri and biramous parapodia. Su-bulate buccal cirri the same length as dorsal tentacular cirri, attached at short cylindrical cirrophores. Cirrophores on anterior ventral surface of neuropodia.

Fifteen pairs of elytra on segments 2, 4, 5, 7, then every second segment until 23, after which on segments 26, 29 and 32. First pair of elytra large, covering the prostomium, modified with a crescent-shaped, transparent, chitinous area. Within the chitinous area there are irregu-larly spaced rounded macrotubercles and more regularly spaced elon-gated, cylindrical macropapillae (Fig. 5B and C). Remaining elytra oval,
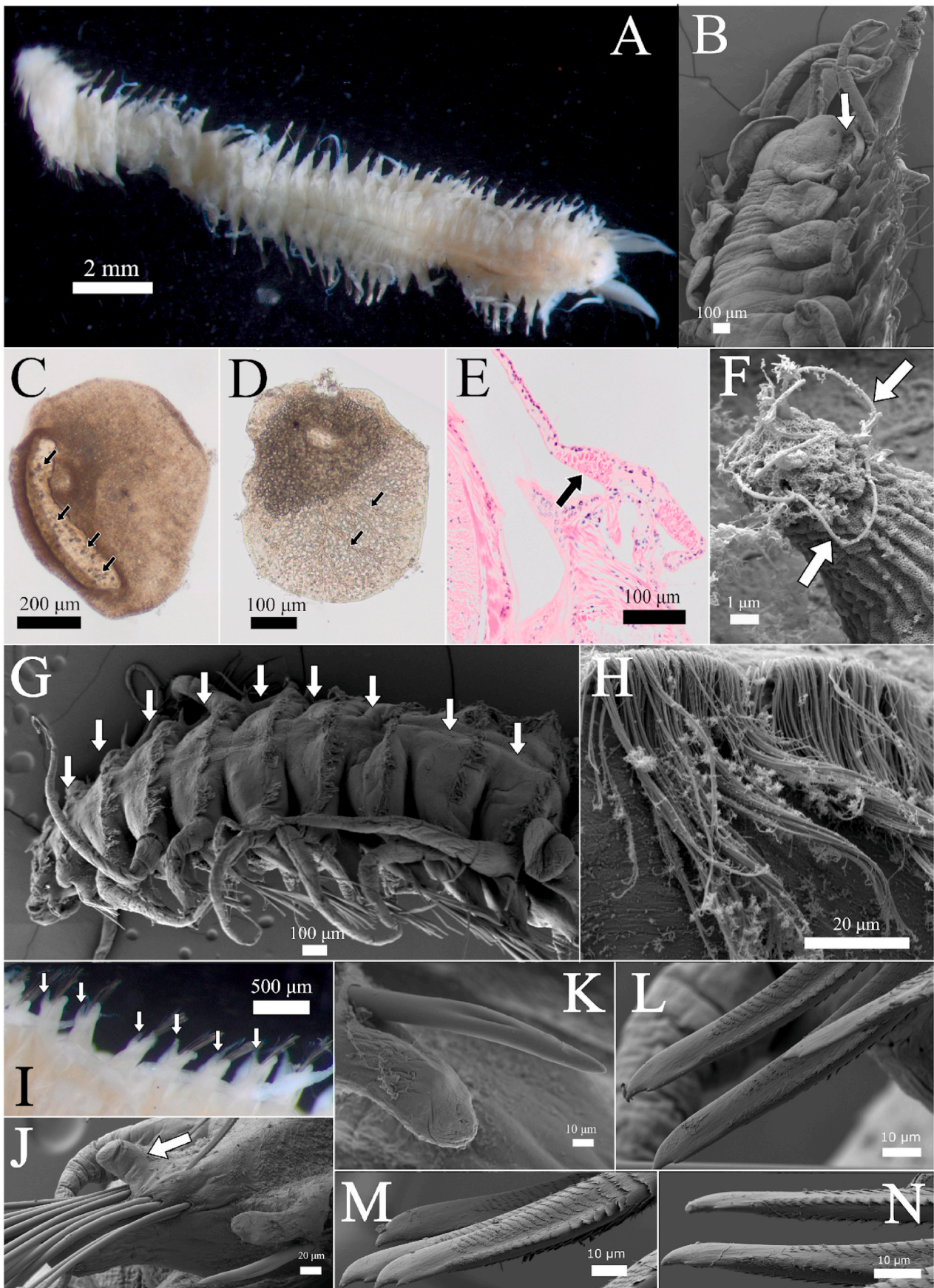
(caption on next page)

Fig. 5. Morphology of *Gorgoniapolynoe pseudocaeciliae* sp. nov. **A**) Full body preserved specimen (USNM 133356) **B**) Anterior region of JC094_ 0602 × 008, showing the modified first elytra (arrow), with the smaller posterior ones**. C**) Modified first elytra with macropapillae (arrows). **D**) The unmodified 2nd elytra with darker area above the elytrophore and the nerves (arrows). **E**) Histological section of the second elytra of JC094_0680 × 004 showing the cup-shaped photocyte-like cells (arrow) concentrated around the elytrophore **F**) Newly observed flagellum-like structures (arrows) emerging from the tips of a macropapillae in the chitinous area of the modified elytra of JC094_0680 × 004. **G**) Cilliary bands present on all segments after the segment containing the last elytra (arrows). **H**) Detail of cilliary bands. **I**) The digitate postsetal lobes of USNM 133356 (arrows). **J**) Posterior of 10th parapodium of JC094_ 0602 × 008, showing the distinct digit-like postsetal neuropodial lobe (arrow). Single notochaeta also visible. **K**) Detail of single robust notochaeta from the same parapodium as H. **L**) Detail of tips of dorsal most neurochaetae. **M**) Detail of tips of mid-neurochaetae. **N**) Detail of tips of ventral most neurochaetae. F, G and H are all from the same neuropodium as H.

smaller than the first pair, with smooth borders curved downwards. Elytra pairs do not touch, leaving the mid-dorsum exposed. Area of the elytra above the elytrophore darker, the rest of the elytra is opaque. Vein-like pattern branching out from the darker area of the elytra (visible under stereoscope). All elytra with randomly and sparsely scattered cylindrical macropapillae across their dorsal surface. Emerging from tips of all macropapillae observed are 3–4 cilia-like structures. These cilia appear to be retractable and can be as long as the width of the elytra. Tips of the cilia flattened and ovoid, these are an artefact of preservation i.e., paddle cilia.

Dorsal cirri present on segments without elytra, long and extending past tips of parapodia. Cirrophores of the dorsal cirri cylindrical, projecting from the posterior side of notopodium. Ventral cirri start from segment 3, with a cylindrical cirrophore. Base of the ventral cirri slightly inflated before tapering, reaching past the tip of the neuropodium. Transverse bands of short cilia present dorsally on random segments. Last 10 segments without elytra with ciliary bands on the dorsal side with cirri, longer and more densely packed compared to other segments (Fig. 5G and H). Small, digitate nephridial papillae from segment six, posterior-ventrally positioned on parapodium. Present on all segments past six but highly reduced in the posterior.

Parapodia biramous, with a subconical acicular notopodium and a neuropodium with a presetal and a postsetal lobe. Presetal lobe of neuropodium diagonally truncated, projecting dorsally. Postsetal lobe shorter, rounded and digitiform, projecting ventrally and away from the neurochaetae (Fig. 5I and J). Projection of pre- and postsetal lobes cause neuropodium to appear bilobed when viewed anteriorly. Postsetal lobe reduced roughly a third of the way down the body. As the postsetal lobe becomes reduced it also takes on the same orientation as the presetal lobe, meaning it can no longer be seen when parapodia viewed from the anterior. There are 1–3 notochaetae, stout, acicular and slightly curved with a small groove on the dorsal side of the curve. Notochaetae positioned anterior to notopodium, longer than it (Fig. 5K). There are 10–15 neurochaetae, as stout as notochaetae with the last third or so becoming quill-like and spinulose. Neurochaetae tips bidentate to varying degrees, with a slight change in form moving from dorsal to ventral. Supraacicular neurochaetae have a slightly hooked, pointed larger tooth and a smaller, rounded secondary tooth (Fig. 5L). Most dorsal of the infraacicular neurochaetae have a more prominent secondary tooth, more pointed than that of supraacicular neurochaetae (Fig. 5M). Ventral most infraacicular neurochaetae more rounded larger tooth with a reduced secondary tooth (Fig. 5N).

Pygidium is a blunt cone, with a pair of anal cirri at the terminus. Bases of the anal cirri closely situated, almost touching. Anal cirri as long or slightly longer than dorsal cirri. Anus ventral to the cirri, protruding slightly.

3.2.6. Histological examination

Histological sections reveal that the darker area corresponds to presence of cup-like cells, possible photocytes (Fig. 5E).

3.2.7. Etymology

The species is named *G. pseudocaeciliae* due to its morphological resemblance to *G. caeciliae*.

3.2.8. Distribution

Gorgoniapolynoe pseudocaeciliae sp. nov. has been reported from Portuguese waters (Pettibone 1991) and in the central Atlantic, on both the east and west side of the Mid-Atlantic Ridge. It has a depth range of between 710 and 2,343 m.

3.2.9. Remarks

The distinct digit-like postsetal lobe on the anterior neuropodium, which projects ventrally to an extent that it can clearly be seen when viewing the neuropodium from the anterior is the character that distinguishes *Gorgoniapolynoe pseudocaeciliae* sp. nov. from *G. caeciliae* (Fig. 3J). The parapodial syntype of *G. caeciliae* (USNM 80098), has a shorter flattened postsetal lobe that lies close to neurochaetae. It is rounded and projects slightly ventrally in anterior segments so that it can just be seen when viewed from anterior. The parapodial syntype was taken from the anterior of the body, so a direct comparison could be made.

Gorgoniapolynoe pseudocaeciliae sp. nov. was previously illustrated by Pettibone (1991) as a morphotype of *Gorgoniapolynoe caeciliae* (USNM 133356). This current study reexamined USNM 133356 and the morphological features concur with the *Gorgoniapolynoe pseudocaeciliae* sp. nov collected for this study. The distinguishing characters that separate this new species from of *G.* cf. *caeciliae* are: (1) the presence of only one type of robust notochaetae, which is curved and smooth; (2) a distinct digit-like postsetal lobe on the anterior neuropodium, which projects ventrally to an extent that it can clearly be seen when viewing the neuropodium from the anterior; and (3) a small, crescent-shaped chitinous area on the modified first elytra pair, that takes up approximately a quarter of the total area of the elytra, as opposed to the one in *G.* cf. *caeciliae*, which is significantly larger. Molecular analyses presented above also support *G. pseudocaeciliae* sp. nov as a distinct species from *G.* cf. *caeciliae*.

4. Discussion

4.1. Addressing Pettibone's (1991) redescription

When Pettibone (1991) redescribed *Gorgoniapolynoe caeciliae* she examined type material USNM 80098, as well as a single individual from the type locality and several specimens from the Western Atlantic. For this current study, all this material was re-examined, along with Fauvel's (1913, 1914) original description and illustrations. The parapodial morphology of the syntype USNM80098 matches that of Pettibone's Western Atlantic specimens but not the individual from the type locality. The modified first elytra were never mentioned in any of the literature until Pettibone (1991), so we do not know what characteristics the type material had. Additionally, the original descriptions lack detail, however, what little detail within them also matches the characters of Pettibone's Western Atlantic specimens. The parapodia of specimens designated as *G.* cf. *caeciliae* in this current study match those of Fauvel's syntype and those of the Western Atlantic specimens examined by Pettibone.

The error in Pettibone (1991) was the designation of the Eastern Atlantic specimen (USNM 133356) as *G. caeciliae*. Pettibone clearly recognised the morphological differences between USNM 133356 and the Western Atlantic specimens, as she chose to illustrate them but for some reason never addressed this in the text. The morphology of the specimens designated as *G. pseudocaeciliae* sp. nov. in this current study match that of USNM 133356. There is no molecular data available for

the syntype. Given this evidence, USNM 133356 should be redesignated as the holotype of *G. pseudocaeciliae.*

4.2. *Gorgoniapolynoe hidden species diversity*

Our study uncovered hidden species diversity within the genus *Gorgoniapolynoe* and increases the number of species from eight to nine. Differences in the parapodia morphology of *G. pseudocaeciliae* sp. nov. and Fauvels's syntype differentiate it as a distinct and separate species from *G. caeciliae.* (Fig. 5; see remarks in section 3.2). There is also the potential for a further two new Gorgoniapolynoe species. Further in-detail morphological investigation is needed into the individuals known as *Gorgoniapolynoe* 'Indian Ocean' to determine what characters delimitate them from other species in this genus. Additionally, the specimens designated here as *G.* cf. *caeciliae* may represent another new species, however given the problems with the current description for *G. caeciliae,* confirmation or refutation of this is impossible without a detailed re-examination of the species as a whole. Furthermore, there is a high genetic diversity within *G.* cf. *caeciliae,* to the extent that it may be a cryptic species complex comprising of two morphologically non-differentiable species i.e., *G.* cf. *caeciliae* MOTU 1 and MOTU 2. While no morphological differences were observed it could be possible that colouration in the living species may discriminate between the two MOTUs. This has shown to be the case in other marine annelids (Nygren and Pleijel, 2011; Pleijel et al., 2009). As all specimens examined here had lost their colouration due to preservation it was impossible to tell if this was the case and highlights the need to image and record colouration at time of collection. More genetic data from additional individuals is needed to determine if what is observed in this study was intraspecific variation or if *G.* cf. *caeciliae* is in fact a cryptic species complex.

Cryptic species have been uncovered within many marine annelid groups using molecular techniques (Grassle and Grassle 1976; Nygren and Pleijel 2011; Nygren 2014 and references within; Borda et al., 2015; Álvarez-Campos et al., 2017; Nygren et al., 2018; Simon et al., 2019). According to Kvist (2016) there is an intraspecific distance range of 0–37% of the *COI* gene across all marine annelids, however, the median genetic distance was 0.79%. Kvist acknowledged that the wide intra-specific distance found may be a result of wrongly identified or undis-covered cryptic species within Genbank, an opinion with which we concur. Other annelid taxa studies have found intraspecific divergence of *COI* to be less than 2% (Brasier et al., 2016; Carr et al., 2011; Drake et al., 2007; Nygren et al., 2018). The interspecific distances in species of the genus *Gorgoniapolynoe* were between 10 and 15% for all pairwise comparisons, which are similar to the distances recorded by Brasier et al. (2016) and Nygren et al. (2018). The mean distance between *G. caeciliae* MOTU 1 and MOTU 2 of 7% is high for intraspecific distance but also is low for interspecific distance based on the aforementioned studies, hence our hesitancy to divide them into two different species without more data.

Gorgoniapolynoe corralophila is distinct within the genus as it is the only species described which has three pairs of anterior modified elytra (Pettibone 1991). It also has distinct large notochaeta with spinose rows. These differences were enough for Britayev et al. (2014) to recommend that the species be moved into its own genus. The positioning of *G. corralophila* within the phylogenetic tree presented here (Fig. 3), along with the discovery of the similar (although much smaller) noto-chaeta in the *G.* cf. *caeciliae* complex would suggest that *G. corralophila* is correctly placed within this genus.

4.3. *Novel morphological features in Gorgoniapolynoe*

On the elytra of all the specimens analysed using SEM, we observed macropapillae bearing 3–4 cilia-like structures with a distal end shaped like a golf club (Figs. 4F and 5F) The shape of the distal end of the cilia is an artefact of preservation. They are referred to as "paddle cilia" or "discocilia" and are believed to form when the fixation method causes

the axoneme to coil within a distal expansion of the ciliary membrane (Short and Tamm, 1991). Some of these cilia were observed to be many times longer than the papillae from which they emerged, longer than the width of the elytra in some cases and potentially retractable (Figs. 4F and 5F). To our knowledge, these cilia emerging from the elytra have not been observed on any other member of *Gorgoniapolynoe.* The only other record of similar structures in a polynoid is *Pholoe minuta* (Fabricius, 1780), a member of the Sigalionidae (subfamily Pholoinae) in the sub-order Aphroditiformia, where cilia-like structures with basal collars were described on the tips of their elytral papillae (Heffernan, 1990). The cilia-like structures of *P. minuta* were hypothesized to be involved in respiration and sensory function. Similarly, we suggest that the cilia in *Gorgoniapolynoe* might have a function in respiration. Segrove (1938) observed and documented epidermal ciliated bands on several different marine annelids. These bands of cilia were observed to produce currents over the surface of the body and were hypothesized to aid respiration via gas exchange through the epidermis. Lwebuga-Mukasa (1970) similarly observed ciliated bands on the polynoid *Halosydna brevisetosa* Kinberg, 1856 and agreed with Segrove (1938) that they probably performed a function in respiration. Cilia on the parapodia create a lateral flow that draws water in under the elytra, where bands on the dorsal surface of the animal further direct this flow posteriorly. No epidermal cilia were observed on the parapodia of *Gorgoniapolynoe,* although some were observed in bands across the dorsal side of elytra-free segments. The cilia emerging from the elytra may provide a similar function to those observed in other species in keeping water circulating within their tunnels. *Gorgoniapolynoe* tunnels are open-ended and the higher density of ciliated papillae on the first elytra could be to create an initial inflow current, while the epidermal ciliated bands observed on the posterior segments may create an outflow. Circulating water through the tunnel in this way would help cutaneous respiration and also function in keeping the tunnel clean, a secondary function suggested by Segrove (1938) and Lwebuga-Mukasa (1970).

Alternatively, the macropapillae with the cilium structures might be involved in the emittance of bioluminescence in combination with the photocytes we detected in our histological analysis (Figs. 2E and 3E). Bioluminescence produced by photocytes has already been described in other polynoids (Nicol 1953; Bassot and Nicolas 1995; Kirkegaard 2001; Taboada et al., 2020a) and macrotubercles present on the elytra could act as refractory prisms thus amplifying the luminescent effect (Nicol 1953; Bassot and Nicolas 1995; Plyuscheva and Martin, 2009). Biolu-minescence in polynoids has been suggested to be used as a warning or distracting mechanism allowing the animal to escape when attacked by a potential predator (Nicol, 1953; Plyuscheva and Martín, 2009), but more recently, it has also been suggested to be used by *Neopolynoe chondrocladiae* (Fauvel, 1943) as a lure for prey (Taboada et al. 2020a). *Neopolynoe chondrocladiae* is an obligate symbiont of two deep-sea carnivorous sponges of the genus *Chondrocladia* that might use biolu-minescence to increase chances of getting more preys, which would benefit both the symbiont and the host sponge (Taboada et al., 2020a; Taboada et al., 2020b). Similarly, we propose that bioluminescence in members of the genus *Gorgoniapolynoe* could be either linked to dissuading potential predators to both the host and the symbiont and/or to attract a greater amount of prey for both partners. In any case, further experiments should be conducted to confirm our hypothesis and also to investigate whether the host octocorals where *Gorgoniapolynoe* are found do have bioluminescent capabilities, as recently described for several deep-sea anthozoans from the coast of California (Bessho-Uehara et al., 2020).

4.4. *Molecular connectivity and dispersal in Gorgoniapolynoe spp.*

Our demographic results conducted on two species of *Gorgoniapoly-noe* agreed in suggesting that there is a certain degree of molecular connectivity between locations separated hundreds to thousands of kilometres. This is especially true for the case of *G. pseudocaeciliae* sp.

nov., where we found three haplotypes shared between the East and West Atlantic seamounts, crossing the Mid-Atlantic Ridge (Fig. 2G). The Mid-Atlantic Ridge (MAR) has been shown to act as a barrier to dispersal and connectivity for some abyssal species (Bober et al., 2018; Boyle, 2011). However, for taxa that are upper bathyal or have highly mobile adults the barrier appears to be more permeable (Coscia et al., 2018; Shields et al., 2013; White et al., 2011; Zardus et al., 2006). Shields et al. (2013) found there to be a level of connectivity between populations of *Eunoe bathydomus* (Ditlevsen, 1917), a commensal polynoid associated with holothurian *Deima validum* Théel, 1879, on either side of the MAR. However, the populations sampled by Shields et al. (2013) were from along the axial trough of the ridge separated by less than 300 km, with east and west populations separated by less than 70 km. Their hosts are also highly mobile and may take long migrations between food-rich areas, thus facilitating gene flow in the polynoids. *Gorgoniapolynoe* are assumed to be broadcast spawners, with relatively high fecundity, with >3,000 eggs recorded in a single female (Eckelbarger et al., 2005). It is therefore assumed that they have a pelagic larval stage which could potentially facilitate the connectivity we report here.

The larval dispersal between the two basins may be aided by the presence of fracture zones that transverse the ridge, particularly the Vema Fracture Zone (VFZ), north of Vema Seamount and Fifteen-Twenty Fracture Zone FTFZ, north-east of Vayda seamount. There is an exchange of waters between the two basins through the VFZ, Antarctic Bottom Water flows eastward, above which North Atlantic Deep Water flows westward (Devey et al., 2018). These offset fractures may also aid in disrupting topographic steering, whereby strong currents are forced to run parallel to the ridge, carry larvae along the ridge and prevent them crossing over it (Young et al., 2008).

Connectivity between widely separated locations at similar bathymetric depths is common in the marine realm but individuals separated vertically by only 100s of metres can have limited or no connectivity (Etter et al., 2005; France and Kocher, 1996; Rex and Etter, 2010; Roy et al., 2012; Taylor and Roterman, 2017; Zardus et al., 2006). It is most likely that this differentiation by depth is a result of the strong vertical environmental gradients e.g. temperature and pressure (Rex and Etter, 2010).

The *Gorgoniapolynoe* in this study went against the common finding of depth being a strong structuring factor, with both species showing no significant structure with depth. In particular, the three largest shared haplotypes in *G. pseudocaeciliae* were found across a depth range of 1600 m (Fig. 3). It may be that having the ability to colonise multiple different host species has increased their odds of settlement across a wide depth range. Lattig et al. (2016) investigated the population structure of *Iphitime cuenoti* Fauvel (1914) (Dorvilleidae) a polyxenous symbiont associated with brachyuran crabs. The results revealed little genetic structure that was independent of their crab hosts. Having multiple hosts, across a 600 m depth range appears to facilitate gene flow and prevent structure. If along with multiple host species, *Gorgoniapolynoe* have a long pelagic larval duration and an ability to tolerate the environmental factors associated with depth, then this would explain the lack of structure associated with depth and distance and explain their wide geographic range in the Atlantic (Lester et al., 2007). The significant genetic variation found on individual hosts suggests that the individual worms are not closely related and that recruitment of worms to the host may be continuous.

5. Conclusion

The current investigation, using a combined morphological and molecular approach, has increased known diversity within *Gorgoniapolynoe* by describing a new species, *Gorgoniapolynoe pseudocaeciliae* sp. nov.. The molecular analysis has uncovered a potentially new species from the deep Indian Ocean previously identified as *G. caeciliae* (Serpetti et al., 2017), and has revealed a wide genetic diversity within *G.* cf. *caeciliae* from the Equatorial Atlantic. We suggest that a complete

reinvestigation into the *G. caeciliae* as a whole is needed. We have uncovered connectivity across large distances and, unusually for the deep-sea, across a wide bathymetric range. Our study highlights again the need to utilize molecular methods in combination with detailed morphological and ecological investigations (Dayrat, 2005) to reinvestigate species with unusually wide ranges and/or having an unusually high number of known hosts, as was the case for *G. caeciliae*. Only with this integrative approach will taxonomy be able to uncover and describe the true diversity of deep-sea life.

Declaration of competing interest

The authors declare that they have no known competing financial interests or personal relationships that could have appeared to influence the work reported in this paper.

Appendix A. Supplementary data

Supplementary data to this article can be found online at https://doi.org/10.1016/j.dsr.2022.103804.

References

Altschul, S.F., Gish, W., Miller, W., Myers, E.W., Lipman, D.J., 1990. Basic local alignment search tool. J. Mol. Biol. 215, 403–410. https://doi.org/10.1016/S0022-2836(05)80360-2.

Álvarez-Campos, P., Giribet, G., Riesgo, A., 2017. The Syllis gracilis species complex: a molecular approach to a difficult taxonomic problem (Annelida, Syllidae). Mol. Phylogenet. Evol. 109, 138–150.

Bandelt, H.-J., Forster, P., Rohl, A., 1994. Median-joining networks for inferring intraspecic phylogenies. Mol. Biol. 16, 37–48. https://doi.org/10.1093/oxfordjournals.molbev.a026036.

Barnich, R., Beuck, L., Freiwald, A., 2013. Scale worms (Polychaeta: Aphroditiformia) associated with cold-water corals in the eastern Gulf of Mexico. J. Mar. Biol. Assoc. U. K. 93, 2129–2143. https://doi.org/10.1017/S002531541300088X.

Bassot, J.-M., Nicolas, M.-T., 1995. Bioluminescence in scale-worm photosomes: the photoprotein polynoidin is specific for the detection of superoxide radicals. Histochem. Cell Biol. 104, 199–210.

Bessho-Uehara, M., Francis, W.R., Haddock, S.H.D., 2020. Biochemical characterization of diverse deep-sea anthozoan bioluminescence systems. Mar. Biol. 167, 114. https://doi.org/10.1007/s00227-020-03706-w.

Bober, S., Brix, S., Riehl, T., Schwentner, M., Brandt, A., 2018. Does the Mid-Atlantic Ridge affect the distribution of abyssal benthic crustaceans across the Atlantic Ocean? Deep Sea Res. Part II Top. Stud. Oceanogr. 148, 91–104. https://doi.org/10.1016/j.dsr2.2018.02.007.

Borda, E., Kudenov, J.D., Chevaldonné, P., Blake, J.A., Desbruyères, D., Fabri, M.-C., Hourdez, S., Pleijel, F., Shank, T.M., Wilson, N.G., Schulze, A., Rouse, G.W., 2015. Cryptic species of Archinome (Annelida: Amphinomida) from vents and seeps. Proceedings. Biol. Sci. 280, 20131876 https://doi.org/10.1098/rspb.2013.1876.

Boyle, E.E., 2011. Evolutionary Patterns in Deep-Sea Mollusks. University of Massachusetts, Boston.

Brasier, M.J., Wiklund, H., Neal, L., Jeffreys, R., Linse, K., Ruhl, H., Glover, A.G., 2016. DNA barcoding uncovers cryptic diversity in 50% of deep-sea Antarctic polychaetes. R. Soc. Open Sci. 3, 160432 https://doi.org/10.1098/rsos.160432.

Britayev, T., Gil, J., Altuna, Á., Calvo, M., Martin, D., 2014. New symbiotic associations involving polynoids (Polychaeta , Polynoidae) from Atlantic waters , with re-description of Parahololepidella greeffi (Augener , 1918). Mem. Mus. Vic. 71, 27–43.

Carr, C.M., Hardy, S.M., Brown, T.M., Macdonald, T.A., Hebert, P.D.N., 2011. A tri-oceanic perspective: DNA barcoding reveals geographic structure and cryptic diversity in Canadian polychaetes. PLoS One 6, 1–12. https://doi.org/10.1371/journal.pone.0022232.

Castelin, M., Williams, S.T., Buge, B., Maestrati, P., Lambourdière, J., Ozawa, T., Utge, J., Couloux, A., Alf, A., Samadi, S., 2017. Untangling species identity in gastropods with polymorphic shells in the genus Bolma Risso, 1826 (Mollusca, Vetigastropoda). Eur. J. Taxon.

Castresana, J., 2000. Selection of conserved blocks from multiple alignments for their use in phylogenetic analysis. Mol. Biol. Evol. 17, 540–552. https://doi.org/10.1093/oxfordjournals.molbev.a026334.

Coscia, I., Castilho, R., Massa-Gallucci, A., Sacchi, C., Cunha, R.L., Stefanni, S., Helyar, S. J., Knutsen, H., Mariani, S., 2018. Genetic homogeneity in the deep-sea grenadier Macrourus berglax across the North Atlantic Ocean. Deep-Sea Res. Part I Oceanogr. Res. Pap. 132, 60–67. https://doi.org/10.1016/j.dsr.2017.12.001.

Dayrat, B., 2005. Towards integrative taxonomy. Biol. J. Linn. Soc. 85, 407–415. https://doi.org/10.1111/j.1095-8312.2005.00503.x.

Devey, C.W., Augustin, N., Brandt, A., Brenke, N., Köhler, J., Lins, L., Schmidt, C., Yeo, I. A., 2018. Habitat characterization of the Vema fracture zone and Puerto Rico trench. Deep Sea Res. Part II Top. Stud. Oceanogr. 148, 7–20. https://doi.org/10.1016/j.dsr2.2018.02.003.

Drake, C.A., McCarthy, D.A., von Dohlen, C.D., 2007. Molecular relationships and species divergence among phragmatopoma spp. (Polychaeta: Sabellariidae) in the Americas. Mar. Biol. 150, 345–358. https://doi.org/10.1007/s00227-006-0373-6.

Dueñas, L., Sánchez, A., 2009. Character lability in deep-sea bamboo corals (Octocorallia, Isididae, Keratoisidinae). Mar. Ecol. Prog. Ser. 397, 11–23.

Eckelbarger, K.J., Watling, L., Fournier, H., 2005. Reproductive biology of the deep-sea polychaete Gorgoniapolynoe caeciliae (Polynoidae), a commensal species associated with octocorals. J. Mar. Biol. Assoc. U. K. 85, 1425–1433. https://doi.org/10.1017/S0025315405012609.

Etter, R., Rex, M.A., Chase, M.R., Quattro, J.M., 2005. Population differentiation decrease with depth in deep-sea bivalves. Evolution (N. Y.) 59, 1479–1491. https://doi.org/10.1111/j.0014-3820.2005.tb01797.x.

Excoffier, L., Lischer, H.E.L., 2010. Arlequin suite ver 3.5: a new series of programs to perform population genetics analyses under Linux and Windows. Mol. Ecol. Resour. 10, 564–567.

Fauvel, P., 1913. Quatrieme note preliminaire sur les Polychetes provenant des campagnes de 1' "///-' rondelle" et de la Princesse- Alice, ou deposees dans le Musee Oceanographique de Monaco. Bulletin de L'Institut Oceanographique, Monaco.

Fauvel, P., 1914. Annélides polychètes non pélagiques provenant des campagnes de l'Hirondelle et de la Princesse-Alice: 1885-1910. Imprimerie de Monaco.

Folmer, O., Hoeh, W.R., Black, M.B., Vrijenhoek, R.C., 1994. Conserved primers for PCR amplification of mitochondrial DNA from different invertebrate phyla. Mol. Mar. Biol. Biotechnol. 3, 294–299.

France, S.C., Kocher, T.D., 1996. Geographic and bathymetric patterns of mitochondrial 16S rRNA sequence divergence among deep-sea amphipods, Eurythenes gryllus. Mar. Biol. 126, 633–643. https://doi.org/10.1007/BF00351330.

Giribet, G., Carranza, S., Baguna, J., Riutort, M., Ribera, C., 1996. First molecular evidence for the existence of a Tardigrada+ Arthropoda clade. Mol. Biol. Evol. 13, 76–84.

Gonzalez, B.C., Martínez, A., Borda, E., Iliffe, T.M., Eibye-Jacobsen, D., Worsaae, K., 2018. Phylogeny and systematics of Aphroditiformia. Cladistics 34, 225–259. https://doi.org/10.1111/cla.12202.

Grassle, J., Grassle, J.F., 1976. Sibling species in the marine pollution indicator Capitella (polychaeta). Science (80-.) 192, 567–569.

Hartmann-Schroder, G., 1985. Polynoecaeciliae Fauvel (Polynoidae), ein mit Korallen assoziierter Polychaet. Mitteilungen aus dem Hambg. Zool. Museum und Inst. 82, 31–35.

Hatch, A.S., Liew, H., Hourdez, S., Rouse, G.W., 2020. Hungry scale worms: phylogenetics of Peinaleopolynoe (Polynoidae, Annelida), with four new species. Zookeys 932, 27–74. https://doi.org/10.3897/zookeys.932.48532.

Heffernan, P., 1990. Ultrastructural studies of the elytra of Pholoe minuta (Annelida: Polychaeta) with special reference to functional morphology. J. Mar. Biol. Assoc. U. K. 70, 545–556.

Higgs, N.D., Attrill, M., 2015. Biases in biodiversity: wide-ranging species are discovered first in the deep sea. Front. Mar. Sci. 2, 61.

Howell, K.L., Hilário, A., Allcock, A.L., Bailey, D.M., Baker, M., Clark, M.R., Colaço, A., Copley, J., Cordes, E.E., Danovaro, R., Dissanayake, A., Escobar, E., Esquete, P., Gallagher, A.J., Gates, A.R., Gaudron, S.M., German, C.R., Gjerde, K.M., Higgs, N.D., Le Bris, N., Levin, L.A., Manea, E., McClain, C., Menot, L., Mestre, N.C., Metaxas, A., Milligan, R.J., Muthumbi, A.W.N., Narayanaswamy, B.E., Ramalho, S.P., Ramirez-Llodra, E., Robson, L.M., Rogers, A.D., Sellanes, J., Sigwart, J.D., Sink, K., Snelgrove, P.V.R., Stefanoudis, P.V., Sumida, P.Y., Taylor, M.L., Thurber, A.R., Vieira, R.P., Watanabe, H.K., Woodall, L.C., Xavier, J.R., 2020. A blueprint for an inclusive, Global deep-sea Ocean decade Field program. Front. Mar. Sci.

Hutchings, P., Kupriyanova, E., 2018. Cosmopolitan polychaetes–fact or fiction? Personal and historical perspectives. Invertebr. Systemat. 32, 1–9.

Katoh, K., Standley, D.M., 2013. MAFFT multiple sequence alignment software Version 7: improvements in performance and usability. Mol. Biol. Evol. 30, 772–780. https://doi.org/10.1093/molbev/mst010.

Kearse, M., Moir, R., Wilson, A., Stones-Havas, S., Cheung, M., Sturrock, S., Buxton, S., Cooper, A., Markowitz, S., Duran, C., Thierer, T., Ashton, B., Mentjies, P., Drummond, A., 2012. Geneious Basic: an integrated and extendable desktop software platform for the organization and analysis of sequence data. Bioinformatics 28, 1647–1649.

Kirkegaard, J.B., 2001. Deep-sea polychaetes from north-west Africa, including a description of a new species of Neopolynoe (Polynoidae). J. Mar. Biol. Assoc. U. K. 81, 391–397. https://doi.org/10.1017/S0025315401004003.

Kumar, S., Stecher, G., Li, M., Knyaz, C., Tamura, K., 2018. MEGA X: molecular evolutionary genetics analysis across computing platforms. Mol. Biol. Evol. 35, 1547–1549.

Kvist, S., 2016. Does a global DNA barcoding gap exist in Annelida? Mitochondrial DNA Part A 27, 2241–2252.

Lanfear, R., Calcott, B., Ho, S.Y.W., Guindon, S., 2012. PartitionFinder: combined selection of partitioning schemes and substitution models for phylogenetic analyses. Mol. Biol. Evol. 29, 1695–1701. https://doi.org/10.1093/molbev/mss020.

Lanfear, R., Frandsen, P.B., Wright, A.M., Senfeld, T., Calcott, B., 2016. PartitionFinder 2: new methods for selecting partitioned models of evolution for molecular and morphological phylogenetic analyses. Mol. Biol. Evol. 34, 772–773.

Lattig, P., Muñoz, I., Martin, D., Abelló, P., Machordom, A., 2016. Comparative phylogeography of two symbiotic dorvilleid polychaetes (Iphitime cuenoti and Ophryotrocha mediterranea) with contrasting host and bathymetric patterns. Zool. J. Linn. Soc. 179, 1–22. https://doi.org/10.1111/zoj.12453.

Leigh, J.W., Bryant, D., 2015. POPART: Full-feature software for haplotype network construction. Methods Ecol. Evol. 6, 1110–1116. https://doi.org/10.1111/2041-210X.12410.

Lester, S.E., Ruttenberg, B.I., Gaines, S.D., Kinlan, B.P., 2007. The relationship between dispersal ability and geographic range size. Ecol. Lett. 10, 745–758. https://doi.org/10.1111/j.1461-0248.2007.01070.x.

Lindgren, J., Hatch, A.S., Hourdez, S., Seid, C.A., Rouse, G.W., 2019. Phylogeny and biogeography of branchipolynoe (Polynoidae, Phyllodocida, Aciculata, Annelida), with descriptions of five new species from methane seeps and hydrothermal vents. Divers. https://doi.org/10.3390/d11090153.

Lwebuga-Mukasa, J., 1970. The role of elytra in the movement of water over the surface of Halosydna brevisetosa (Polychaeta: Polynoidae). Bull. South Calif. Acad. Sci. 69, 154–160.

Macpherson, E., Beuck, L., Freiwald, A., 2016. Some species of munidopsis from the Gulf of Mexico, Florida Straits and Caribbean Sea (Decapoda: Munidopsidae), with the description of two new species. Zootaxa 4137, 405–416.

Martin, D., Aguado, M.T., Fernández Álamo, M.-A., Britayev, T.A., Böggemann, M., Capa, M., Faulwetter, S., Fukuda, M.V., Helm, C., Petti, M.A., Ravara, A., Teixeira, M.A.L., 2021. On the Diversity of Phyllodocida (Annelida: Errantia), with a Focus on Glyceridae, Goniadidae, Nephtyidae, Polynoidae, Sphaerodoridae, Syllidae, and the Holoplanktonic Families. Divers. https://doi.org/10.3390/d13030131.

Martin, D., Britayev, T.A., 2018. Symbiotic polychaetes revisited : an update of the known species and relationships (1998 – 2017). In: Oceanography and Marine Biology: an Annual Review. UCL Press, pp. 371–448.

Martin, D., Britayev, T.A., 1998. Symbiotic polychaetes: review of known species. Oceanogr. Mar. Biol. 36, 217–340.

Molodtsova, T.N., Britayev, T.A., Martin, D., 2016. Cnidarians and their polychaete symbionts. In: Goffredo, S., Dubinsky, Z. (Eds.), The Cnidaria, Past, Present and Future: the World of Medusa and Her Sisters. Springer International Publishing, Cham, pp. 387–413. https://doi.org/10.1007/978-3-319-31305-4_25.

Nicol, Jac, 1953. Luminescence in polynoid worms. J. Mar. Biol. Assoc. U. K. 32, 65–84.

Nygren, A., 2014. Cryptic polychaete diversity: a review. Zool. Scripta 43, 172–183. https://doi.org/10.1111/zsc.12044.

Nygren, A., Parapar, J., Pons, J., Meißner, K., Bakken, T., Kongsrud, J.A., Oug, E., Gaeva, D., Sikorski, A., Johansen, R.A., 2018. A mega-cryptic species complex hidden among one of the most common annelids in the North East Atlantic. PLoS One 13, e0198356.

Nygren, A., Pleijel, F., 2011. From one to ten in a single stroke – resolving the European Eumida sanguinea (Phyllodocidae, Annelida) species complex. Mol. Phylogenet. Evol. 58, 132–141. https://doi.org/10.1016/j.ympev.2010.10.010.

Oug, E., Bakken, T., Kongsrud, J.A., Alvestad, T., 2017. Polychaetous annelids in the deep Nordic Seas: strong bathymetric gradients, low diversity and underdeveloped taxonomy. Deep Sea Res. Part II Top. Stud. Oceanogr. 137, 102–112. https://doi.org/10.1016/j.dsr2.2016.06.016.

Palumbi, S.R., 1996. Nucleic acids II: the polymerase chain reaction. In: Hillis, D.M., Moritz, C., Mable, B.K. (Eds.), Molecular Systematics, pp. 205–247.

Pettibone, M.H., 1991. Polynoids commensal with gorgonian and stylasterid corals, with a new genus, new combinations, and new species (polychaeta: polynoidae: polynoinae). Proc. Biol. Soc. Wash. 104, 688–713.

Pleijel, F., Rouse, G., Nygren, A., 2009. Five colour morphs and three new species of Gyptis (Hesionidae, Annelida) under a jetty in Edithburgh, South Australia. Zool. Scripta 38, 89–99. https://doi.org/10.1111/j.1463-6409.2008.00356.x.

Plyuscheva, M., Martin, D., 2009. On the morphology of elytra as luminescent organs in scale-worms (Polychaeta, Polynoidae). Zoosymposia 2, 379–389.

Puillandre, N., Lambert, A., Brouillet, S., Achaz, G., 2012. ABGD, automatic Barcode gap discovery for primary species delimitation. Mol. Ecol. 21, 1864–1877.

Rambaut, A., Drummond, A.J., 2012. FigTree Version 1.4. 0.

Rambaut, A., Drummond, A.J., Xie, D., Baele, G., Suchard, M.A., 2018. Posterior summarization in bayesian phylogenetics using tracer 1.7. Syst. Biol. 67, 901–904. https://doi.org/10.1093/sysbio/syy032.

Rex, M.A., Etter, R.J., 2010. Deep-sea Biodiversity: Pattern and Scale. Harvard University Press.

Roy, D., Hurlbut, T.R., Ruzzante, D.E., 2012. Biocomplexity in a demersal exploited fish, white hake (Urophycis tenuis): depth-related structure and inadequacy of current management approaches. Can. J. Fish. Aquat. Sci. 69, 415–429. https://doi.org/10.1139/f2011-178.

Rozas, J., Ferrer-Mata, A., Sánchez-DelBarrio, J.C., Guirao-Rico, S., Librado, P., Ramos-Onsins, S.E., Sánchez-Gracia, A., 2017. DnaSP 6: DNA sequence polymorphism analysis of large data sets. Mol. Biol. Evol. 34, 3299–3302. https://doi.org/10.1093/molbev/msx248.

Segrove, F., 1938. 8. An account of surface ciliation in some polychaete worms. Proc. Zool. Soc. Lond. B108, 85–108. https://doi.org/10.1111/j.1096-3642.1938.tb00025.x.

Serpetti, N., Taylor, M.L., Brennan, D., Green, D.H., Rogers, A.D., Paterson, G.L.J., Narayanaswamy, B.E., 2017. Ecological adaptations and commensal evolution of the polynoidae (Polychaeta) in the Southwest Indian Ocean ridge: a phylogenetic approach. Deep Sea Res. Part II Top. Stud. Oceanogr. 137, 273–281. https://doi.org/10.1016/j.dsr2.2016.06.004.

Shields, M.A., Glover, A.G., Wiklund, H., 2013. Polynoid polychaetes of the Mid-Atlantic Ridge and a new holothurian association. Mar. Biol. Res. 9, 547–553. https://doi.org/10.1080/17451000.2012.749992.

Short, G., Tamm, S.L., 1991. On the nature of paddle cilia and discocilia. Biol. Bull. 180, 466–474. https://doi.org/10.2307/1542347.

Simon, C.A., Sato-Okoshi, W., Abe, H., 2019. Hidden diversity within the cosmopolitan species Pseudopolydora antennata (Claparède, 1869)(Spionidae: Annelida). Mar. Biodivers. 49, 25–42.

Simpson, A., Watling, L., 2011. Precious corals (Coralliidae) from north-western Atlantic seamounts. J. Mar. Biol. Assoc. U. K. 91, 369–382. https://doi.org/10.1017/S002531541000086X.

Stamatakis, A., 2014. RAxML Version 8: a tool for phylogenetic analysis and post-analysis of large phylogenies. Bioinformatics 30, 1312–1313.

Stock, J.H., 1986. Cases of hyperassociation in the copepoda (Herpyllobiidae and Nereicolidae). Syst. Parasitol. 8, 71–81. https://doi.org/10.1007/BF00010311.

Struck, T.H., Purschke, G., Halanych, K.M., 2006. Phylogeny of Eunicida (Annelida) and exploring data congruence using a partition addition bootstrap alteration (PABA) approach. Syst. Biol. 55, 1–20.

Taboada, S., Silva, A.S., Neal, L., Cristobo, J., Ríos, P., Álvarez-Campos, P., Hestetun, J. T., Koutsouveli, V., Sherlock, E., Riesgo, A., 2020a. Insights into the symbiotic relationship between scale worms and carnivorous sponges (Cladorhizidae, Chondrocladia). Deep-Sea Res. Part I Oceanogr. Res. Pap. 156, 103191 https://doi.org/10.1016/j.dsr.2019.103191.

Taboada, S., Serra Silva, A., Díez-Vives, C., Neal, L., Cristobo, J., Ríos, P., Hestetun, J.T., Clark, B., Rossi, M.E., Junoy, J., Navarro, J., Riesgo, A., 2020b. Sleeping with the enemy: unravelling the symbiotic relationships between the scale worm Neopolynoe chondrocladiae (Annelida: Polynoidae) and its carnivorous sponge hosts. Zool. J. Linn. Soc. https://doi.org/10.1093/zoolinnean/zlaa146.

Taylor, M.L., Roterman, C.N., 2017. Invertebrate population genetics across Earth's largest habitat: the deep-sea floor. Mol. Ecol. 26, 4872–4896. https://doi.org/10.1111/mec.14237.

Templeton, A.R., Crandall, K.A., Sing, C.F., 1992. A cladistic analysis of phenotypic associations with haplotypes inferred from restriction endonuclease mapping and DNA sequence data. III. Cladogram estimation. Genetics 132, 619–633.

Tu, T.-H., Altuna, A., Jeng, M.-S., 2015. Coralliidae (Anthozoa: Octocorallia) from the INDEMARES 2010 expedition to north and northwest Spain (northeast Atlantic), with delimitation of a new species using both morphological and molecular approaches. Zootaxa 3926, 301–328.

Ván Le, H.L., Lecointre, G., Perasso, R., 1993. A 28S rRNA-based phylogeny of the gnathostomes: first steps in the analysis of conflict and congruence with morphologically based cladograms. Mol. Phylogenet. Evol. 2, 31–51.

Vrijenhoek, R.C., 2009. Cryptic species, phenotypic plasticity, and complex life histories: assessing deep-sea faunal diversity with molecular markers. Deep Sea Res. Part II Top. Stud. Oceanogr. 56, 1713–1723. https://doi.org/10.1016/j.dsr2.2009.05.016.

White, T.A., Fotherby, H.A., Stephens, P.A., Hoelzel, A.R., 2011. Genetic panmixia and demographic dependence across the North Atlantic in the deep-sea fish, blue hake (Antimora rostrata). Heredity 106, 690–699. https://doi.org/10.1038/hdy.2010.108.

Whiting, M.F., 2002. Mecoptera is paraphyletic: multiple genes and phylogeny of Mecoptera and Siphonaptera. Zool. Scripta 31, 93–104.

Whiting, M.F., Carpenter, J.C., Wheeler, Q.D., Wheeler, W.C., 1997. The Strepsiptera problem: phylogeny of the holometabolous insect orders inferred from 18S and 28S ribosomal DNA sequences and morphology. Syst. Biol. 46, 1–68.

Young, C.R., Fujio, S., Vrijenhoek, R.C., 2008. Directional dispersal between mid-ocean ridges: deep-ocean circulation and gene flow in Ridgeia piscesae. Mol. Ecol. 17, 1718–1731. https://doi.org/10.1111/j.1365-294X.2008.03609.x.

Zardus, J.D., Etter, R.J., Chase, M.R., Rex, M.A., Boyle, E.E., 2006. Bathymetric and geographic population structure in the pan-Atlantic deep-sea bivalve Deminucula atacellana (Schenck, 1939). Mol. Ecol. 15, 639–651. https://doi.org/10.1111/j.1365-294X.2005.02832.x.

Zhang, J., Kapli, P., Pavlidis, P., Stamatakis, A., 2013. A general species delimitation method with applications to phylogenetic placements. Bioinformatics 29, 2869–2876.

Zhang, Y., Sun, J., Rouse, G.W., Wiklund, H., Pleijel, F., Watanabe, H.K., Chen, C., Qian, P.-Y., Qiu, J.-W., 2018. Phylogeny, evolution and mitochondrial gene order rearrangement in scale worms (Aphroditiformia, Annelida). Mol. Phylogenet. Evol. 125, 220–231. https://doi.org/10.1016/j.ympev.2018.04.002.